



U.S. DEPARTMENT OF
ENERGY

Office of
Science

DOE/SC-ARM-14-037

Layered Atlantic Smoke Interactions with Clouds (LASIC) Science Plan

P Zuidema	MJ Alvarado
C Chiu	SP DeSzoeki
CW Fairall	G Feingold
SJ Ghan	JM Haywood
P Kollias	ER Lewis
GM McFarguhar	A McComiskey
DB Mechem	J Redemann
DM Romps	DD Turner
H Wang	R Wood
SE Yuter	P Zhu

March 2016



DISCLAIMER

This report was prepared as an account of work sponsored by the U.S. Government. Neither the United States nor any agency thereof, nor any of their employees, makes any warranty, express or implied, or assumes any legal liability or responsibility for the accuracy, completeness, or usefulness of any information, apparatus, product, or process disclosed, or represents that its use would not infringe privately owned rights. Reference herein to any specific commercial product, process, or service by trade name, trademark, manufacturer, or otherwise, does not necessarily constitute or imply its endorsement, recommendation, or favoring by the U.S. Government or any agency thereof. The views and opinions of authors expressed herein do not necessarily state or reflect those of the U.S. Government or any agency thereof.

Layered Atlantic Smoke Interactions with Clouds (LASIC) Science Plan



P Zuidema
C Chiu
CW Fairall
SJ Ghan
P Kollias
GM McFarguhar
DB Mechem
DM Romps
H Wang
SE Yuter
Co-Investigators

MJ Alvarado
SP DeSzoeki
G Feingold
JM Haywood
ER Lewis
A McComiskey
J Redemann
DD Turner
R Wood
P Zhu

March 2016

Work supported by the U.S. Department of Energy,
Office of Science, Office of Biological and Environmental Research

Summary

Southern Africa is the world's largest emitter of biomass-burning (BB) aerosols. Their westward transport over the remote southeast Atlantic Ocean colocates some of the world's largest atmospheric loadings of absorbing aerosol with the least examined of the Earth's major subtropical stratocumulus decks. Global aerosol model results highlight that the largest positive top-of-atmosphere forcing in the world occurs in the southeast Atlantic, but this region exhibits large differences in magnitude and sign between reputable models, in part because of high variability in the underlying model cloud distributions. Many uncertainties contribute to the highly variable model radiation fields: the aging of shortwave-absorbing aerosol during transport, how much of the aerosol mixes into the cloudy boundary layer, and how the cloudy boundary layer adjusts to smoke-radiation and smoke-cloud microphysical interactions. In addition, the ability of the BB aerosol to absorb shortwave radiation is known to vary seasonally as the fuel type on land changes.

The goal of the LASIC campaign, or Layered Atlantic Smoke Interactions with Clouds, is to improve our understanding of aged carbonaceous aerosol, its seasonal evolution, and the mechanisms by which clouds adjust to the presence of the aerosol. The observational strategy centers on deploying the first Atmospheric Radiation Measurement (ARM) Climate Research Facility Mobile Facility (AMF1) cloud, aerosol, and atmospheric profiling instrumentation to Ascension Island, which is located within the trade-wind shallow cumulus regime (15°W, 8°S) almost 2000 km west of continental Africa. The location is within the latitude zone of the maximum outflow of aerosol, with the deepening boundary layer known to entrain free-tropospheric smoke. The primary activities for LASIC are 1) to improve current knowledge of aged BB aerosol and its radiative properties as a function of the seasonal cycle; 2) to use surface-based remote sensing to sensitively interrogate the atmosphere for the relative vertical location of aerosol and clouds; 3) to improve our understanding of the cloud adjustments to the presence of shortwave-absorbing aerosol within the vertical column, both through aerosol-radiation and through aerosol-cloud interactions; and 4) to aid low-cloud parameterization efforts for climate models.

The measurements will span the June 1, 2016 to October 31, 2017 timeframe, encompassing two July-to-October BB seasons. The August to September 2016 months will include an intensive operational period (IOP) with 8x/daily radiosondes, overlapping with the U.K. Cloud-Aerosol-Radiation Interactions and Forcing (CLARIFY) and National Aeronautic and Space Administration Observations of Aerosols above Clouds and their Interactions (NASA-ORACLES) aircraft 2016 deployments sharing similar objectives, based in Namibia. A more modest secondary instrumentation suite (radar, lidar, spectrometer, AERONET) will be placed on St. Helena Island (5°W, 15°S), which is located upwind of Ascension Island within the boundary-layer flow and downwind within the free-tropospheric aerosol flow, in 2016 through UK-US-DOE cooperation. In 2017, LASIC will overlap with NASA ORACLES-2017. Ascension Island is already an AERONET site and hosts a U.K./U.S. military airfield. A comprehensive modeling plan will use the observations to further test LASIC hypotheses.

Colocated smoke and clouds over the remote ocean represent a regime of significant climatic importance that has not yet been interrogated with comprehensive surface-based measurements. Ascension Island is strategically located for the collection of observations that will be helpful in resolving current uncertainties about the aging and transport of smoke and the low-cloud response. These processes affect the spatial and vertical distribution of the Earth's radiative balance at a location with important cloud feedback to climate. The long-term, high-time-resolution measurements from a DOE AMF1 deployment provide a stringent test for global aerosol models.

Acronyms and Abbreviations

ABE	Aerosol Best Estimate
ACSM	Aerosol Chemistry Speciation Monitor
AEROCOM	Aerosol Comparisons between Observations and Models – an international aerosol modeling intercomparison initiative focused on understanding global aerosol and its impact on climate
AMF	ARM Mobile Facility
AMF1	first ARM Mobile Facility
AERONET	Aerosol Robotic Network
AMSR-E	Advanced Microwave Scanning Radiometer-E
AOD	aerosol optical depth
ARM	Atmospheric Radiation Measurement
ARSCL	Active Remote Sensing of Cloud Locations
BB	biomass burning
BBC	British Broadcasting Corporation
BC	black carbon
CALIOP	Cloud Aerosol Lidar with Orthogonal Polarization
CAM5	Community Atmosphere Model version 5
CAP-MBL	Clouds, Aerosols, Precipitation in the Marine Boundary Layer
CCN	cloud condensation nuclei
CERES	Clouds and Earths' Radiant System
CESM	Community Earth System Model
CLARIFY	Cloud-Aerosol-Radiation Interactions and Forcing
CloudSat	a NASA satellite that studies the role of clouds and aerosols in regulating Earth's weather, climate, and air quality
CMIP	Coupled Model Intercomparison Project – a standard experimental protocol for studying the output of coupled atmosphere-ocean general circulation models
DOE	U. S. Department of Energy
ERA	European Reanalysis of the Global Climate System – an atmospheric reanalysis of the 20 th century developed by the European Centre for Medium-Range Weather Forecasts
FLEXPART-WRF	FLEXible PARTicle dispersion model – a combination of Weather Research and Forecasting meteorological fields with a Lagrangian particle dispersion model

GNDRAD	Ground Radiation – an ARM collection of radiometers that provides continuous measurements of broadband shortwave (solar) and longwave (infrared) irradiances for upwelling atmospheric components
GPCI	GEWEX/WGNE Pacific Cross-section Intercomparison – a Global Energy and Water Cycle Experiment/Working Group for Numerical Experimentation program to evaluate climate and weather prediction models in the tropics and sub-tropics, using satellite observations
HSRL	high-spectral-resolution lidar
HYSPLIT	Hybrid Single Particle Lagrangian Integrated Trajectory Model – a NOAA Air Resources Laboratory system for computing simple air parcel trajectories to complex dispersion and deposition simulations
INDOEX	Indian Ocean Experiment – an NCAR field study of the role of anthropogenic aerosols in climate change that was conducted from January through March 1999 over the tropical Indian Ocean
IOP	intensive operational period
KASACR	K-Band Scanning Cloud Radar
Ka/W-SACR	Ka/W-Scanning ARM Cloud Radars
LASIC	Layered Atlantic Smoke Interactions with Clouds
LBLRTM	Line-By-Line Radiative Transfer Model
LES	large-eddy simulation
LWP	liquid water path
MAM	modal aerosol module developed for the CAM5
MAOS	Mobile Aerosol Observing System
MAOS-A	MAOS-Aerosol
MAOS-C	MAOS-Chemistry
MFRSR	Multifilter Rotating Shadowband Radiometer
MMF	multi-scale modeling framework
MODIS	Moderate Resolution Imaging Spectroradiometer
MPL	micropulse lidar
MPLNET	Micro-Pulse Lidar Network – a NASA network of MPL systems that measures aerosol and cloud vertical structure continuously, day and night, over long periods
MWRHF	Microwave Radiometer, High Frequency
MWR3C	Microwave Radiometer, 3-Channel
NASA	National Aeronautics and Space Administration

NASA-ORACLES	National Aeronautics and Space Administration Observations of Aerosols above Clouds and their Interactions
NCAR	National Center for Atmospheric Research
NCCN	North Coast and Cascades Network – a long-term climate monitoring program run by the U.S. National Park Service
NFOV	Narrow Field of View – an ARM instrument
NIR	near-infrared regions
NOAA	National Oceanic and Atmospheric Administration
NSF	National Science Foundation
NSF ONFIRE	ObservationNs of Fire’s Impact on the southeast atlantic Region
OCEANET	OceaNET – a European Commission research project examining floating offshore wind and wave energy
PASS	Photo-Acoustic Soot Spectrometer
PCASP	Passive Cavity Aerosol Spectrometer Probe
PI	principal investigator
PNNL	Pacific Northwest National Laboratory
POM	particulate organic matter
POP	precipitation of probability
PSAP	Particle Soot Absorption Photometer
RICO	Rain In Cumulous over the Ocean
RIPBE	Radiatively Important Parameters Best Estimate
RWP	Radar Wind Profiler
SAFARI-UK	Southern African Regional science Initiative
SAS-He	Solar Array Spectrometer – Hemispheric
SAS-Ze	Solar Array Spectrometer – Zenith
SCM	single-column model
SEBS	surface energy balance system
SGP	Southern Great Plains ARM site
SKYRAD	Sky Radiation – an ARM collection of radiometers providing continuous measurements of broadband shortwave (solar), longwave (infrared), and ultraviolet irradiances for downwelling atmospheric components
SMPS	Scanning Mobility Particle Sizer
SOA	Service-Oriented Architecture – an Oracle application and service integration software suite

SPOP	susceptibility of POP
SSA	single-scattering albedo
SST	sea surface temperature
UHSAS	Ultra-High-Sensitivity Aerosol Spectrometer
UK	United Kingdom
US	United States
VAMOS	Variability of the American Monsoon System
VAPs	value-added products
VARANAL	Constrained Variational Analysis – an ARM value-added product
VBS	Volatility Basis Set
VOCALS	VAMOS Ocean-Cloud-Atmosphere-Land Study
WACR	W-Band Zenith Cloud Radar
WRF	Weather Research and Forecasting Model
WRF-Chem	Weather Research and Forecasting Model coupled with Chemistry
WSACR	W-Band Scanning Cloud Radar

Contents

Summary	iii
Acronyms and Abbreviations	iv
1.0 Introduction	1
1.1 Smoke Radiation and Composition.....	3
1.2 Smoke-Cloud Interactions.....	4
2.0 LASIC Activities, Goals, Hypotheses, and Instrument Tables.....	6
2.1 Activities	6
2.2 Goals	6
2.3 Instrumentation.....	7
3.0 Specific Objectives	9
3.1 Characterizing Aged Carbonaceous Aerosol (H1)	9
3.2 Accurate Identification of Aerosol-Cloud Vertical Structure (supports H2, H3 and H4)	10
3.3 Cloud Adjustments to Aerosol-Radiation and Aerosol-Cloud Interactions (H2, H3).....	11
3.4 Distinguishing Aerosol from Meteorological Effects (H2, H4)	13
3.5 Measurements that Span the Full Annual Cycle, and Low-Cloud Model Parameterization Development Support (H2, H4)	15
4.0 Site Description, Planning, Value-Added Products, and Collaborations	16
4.1 Site Description.....	16
4.2 Related Campaigns.....	18
4.3 Priority Value-Added Products and Guest Instrumentation.....	19
5.0 Modeling Plan.....	21
6.0 Relevance to U.S. Department of Energy.....	23
7.0 References	25

Figures

1.	The September-mean sea-surface temperature and cloud-fraction highlights the large southeast Atlantic stratocumulus region in comparison to the southeast Pacific.	1
2.	Estimates of the August-September top-of-atmosphere direct radiative forcing from 12 global aerosol models	2
3.	During September, 600 hPa winds escort the BB aerosol from fires in continental Africa westward over the entire south Atlantic stratocumulus deck.	3
4.	From left to right: vertical profiles of PCASP accumulation-mode aerosol concentration and the nephelometer scattering coefficient at 0.55 micron indicate aerosol concentrations exceeding 500 cm ⁻³ in the boundary layer.	4
5.	Precipitation susceptibility as a function of LWP in AMF data (with respect to N_{CCN}) and from VAMOS Ocean-Cloud-Atmosphere-Land Study (VOCALS) and RICO large-eddy simulation (LES) data sets.....	5
6.	CALIOP snapshots of 532-micron backscattered intensity near Ascension Island suggest a range of cloud-aerosol interactions.....	10
7.	Monthly-mean profiles of atmospheric potential temperature, relative humidity, and mixing ratio clearly highlight the warmer, deeper, and more moist boundary layer at Ascension Island compared to St. Helena.....	14
8.	The annual cycle in (left) cloud amount and (right) LWP over the 10° to 20° S, 0° to 10° E region in CMIP5 models and observations.....	15
9.	Views of Ascension Island.	17
10.	Ascension Island layout of instrumentation.....	18
11.	CMIP3 Intermodel regression of the local cloud feedback upon the global mean cloud feedback..	22

Tables

1	AMF1 Instrumentation	7
2	U.K. Met Office/UMiami/NASA Instrumentation upon St. Helena, fall 2016 only.	19
3	Guest instrumentation, anticipated (black) and desired (blue).	210

1.0 Introduction

The southeast Atlantic net cloud radiative forcing attains a global maximum on par with that of the southeast Pacific (Lin et al. 2010; Figure 1). South-easterly near-surface winds stream toward the equator as part of their anticyclonic rotation around the south Atlantic sea level pressure high. In contrast, lower free-tropospheric winds (600-700 hPa) are primarily driven by a deeper anticyclone based over southern Africa. These warm winds combine with the cool sea surface temperatures to encourage the formation of a large stratocumulus deck, transitioning to year-round trade-wind shallow cumulus at the location of Ascension Island (14.5° W, 8° S; Figure 1). This remote but populated volcanic island is the location selected for the first Atmospheric Radiation Measurement (ARM) Climate Research Facility Mobile Facility (AMF1) deployment from June 1, 2016 to October 31, 2017.

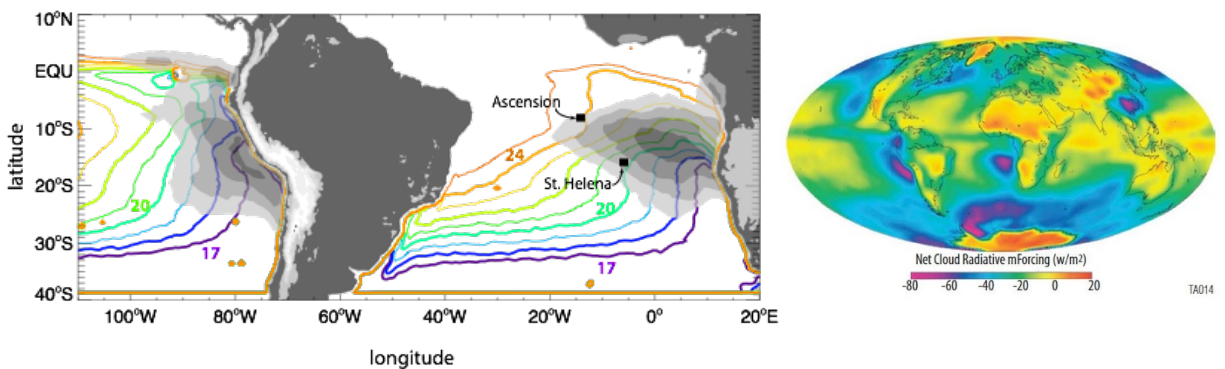


Figure 1. Left-hand panel: The September-mean sea-surface temperature and cloud-fraction highlights the large southeast Atlantic stratocumulus region in comparison to the southeast Pacific and indicates the AMF1/MAOS deployment base of Ascension Island and partner St. Helena. The figure illustrates sea-surface temperatures from 1998 to 2013 via Thematic Microwave Imager (labeled colored contour lines in degrees Celsius) and low-cloud fraction from 2000 to 2012 Moderate Resolution Imaging Spectroradiometer (MODIS; grey shading spans 0.6-1). Land topography shown in 1 km height increments. Right-hand panel: Clouds and Earths' Radiant System (CERES) annual-mean net cloud radiative forcing for March 2000 to February 2001, from <http://npp.gsfc.nasa.gov>.

An unexamined low-cloud regime for the U.S. Department of Energy's (DOE's) ARM Climate Research Facility is shallow cloud interactions with aerosols resulting from biomass burning. Such aerosols absorb as well as scatter shortwave radiation and shortwave-absorbing aerosols are capable of providing a positive impact on climate (a warming), in contrast to the cooling provided by aerosols, such as sulfate particles, that only scatter shortwave radiation. The separate contribution of biomass-burning (BB) aerosols to the global climate is highlighted within the Technical Summary of the most recent 2014 Intergovernmental Panel on Climate Change report, where the global direct radiative forcing is estimated at +0.2 to -0.2 W m⁻² (Boucher et al. 2013). The contribution to regional climate, particularly over the southeast Atlantic, is much stronger.

As shown in Figure 2, global aerosol model estimates of the aerosol direct radiative effect vary widely, even when the aerosol radiative properties are identically prescribed. The model intercomparison AeroCom project, an open call to aerosol modeling groups to compare their models using identical setups, has focused on providing comprehensive assessments of the aerosol life cycle in participating models

(Kinne et al. 2013; Schultz et al. 2006; Stier et al. 2013; Myrhe et al. 2013). The AeroCom top-of-atmosphere results demonstrate that, in the mean, the largest positive top-of-atmosphere forcing in the world occurs in the southeast Atlantic, but this region also exhibits large differences in magnitude and sign between reputable models. This is also consistent with high variability in the underlying model cloud distributions (Stier et al. 2013) and differences in the aerosol vertical distribution (Koffi et al. 2012). The AeroCom project is planning a future activity with a focus on BB aerosol effects. De Graaf et al. (2012) used high-spectral-resolution satellite data to show that the direct radiative effect of BB aerosol over clouds in the southeastern Atlantic region can exceed $+130 \text{ W m}^{-2}$ instantaneously, and $+23 \text{ W m}^{-2}$ in the monthly mean (de Graaf et al. 2014). These values are far higher than those diagnosed in climate models in which monthly-mean regional values reach only $+5 \text{ W m}^{-2}$ (Figure 2). Underrepresented underlying low cloud albedo in the climate models provides one plausible explanation.

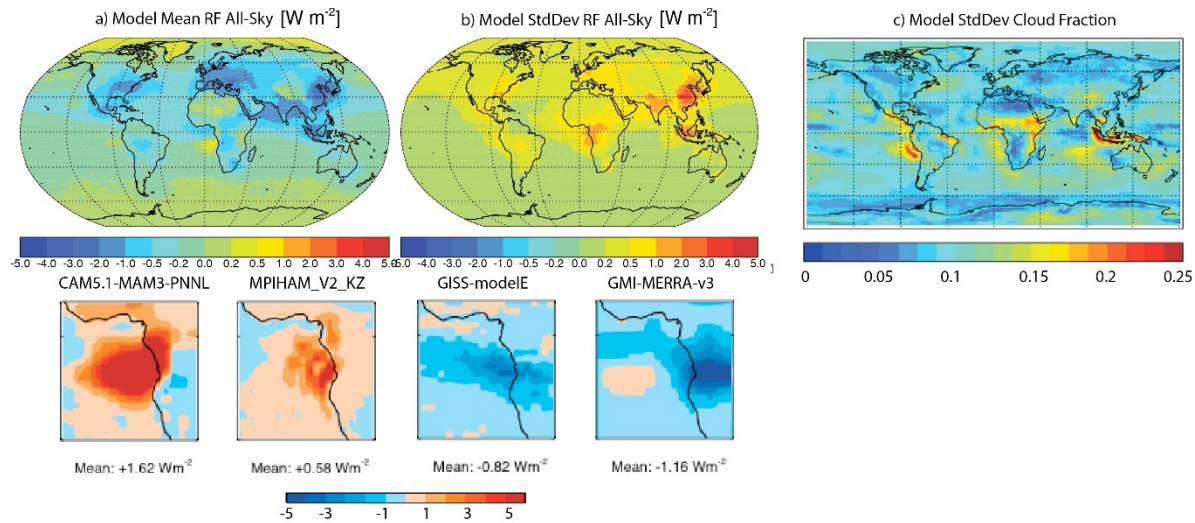


Figure 2. Estimates of the August-September top-of-atmosphere direct radiative forcing from 12 global aerosol models with prescribed radiative properties (Stier et al. 2013).

Ascension and St. Helena islands are subject to the free-tropospheric BB emissions emanating from Africa (Figure 3). The largest consumption of biomass by fire in the world occurs in Africa (van der Werf et al. 2006, 2010; Granier et al. 2011), with the global majority of aerosols overlying clouds occurring in the southeast Atlantic (Waquet et al. 2013). The BB aerosol created during these fires extends well into the trade-wind cumulus region, where the deepening boundary layer and subsiding aerosol layer are more likely to directly interact (Figure 3, inset). Few observations from the remote southeast Atlantic are available, however, because satellite measurements are not yet able to determine the extent to which aerosol is entrained into the boundary layer. Vertical profile data from one U.K. Met Office research flight to Ascension Island as part of the Southern African Regional science Initiative (SAFARI-UK) in 2000 show enhanced aerosol concentrations within the boundary layer (Figure 4). Longer-term aerosol statistics, such as data that will be available from the DOE AMF1 platform, will provide definitive climatology information both at the surface and of the vertical structure, thus placing such anecdotal evidence on stronger footing.

1.1 Smoke Radiation and Composition

At the top of the atmosphere, the direct radiative effect of the BB aerosol is positive (i.e., a warming) when the aerosol is located above a bright cloud deck, and negative (i.e., a cooling) when above a dark ocean surface (Remer 2009). For a typical BB aerosol single-scattering albedo (SSA) of 0.9, the cloud fraction above which the aerosol exerts an overall warming is approximately 0.4 (Russell et al. 1997; Abel et al. 2005; Chand et al. 2009; Seidel and Popp 2012), based on plane-parallel radiative transfer calculations constrained by satellite data. It is also worth emphasizing that small changes in aerosol SSA have a disproportionate impact on the sign of the net top-of-atmosphere radiative forcing (Haywood and Shine, 1995; Haywood et al., 2004; Leahy et al., 2007; Magi et al., 2008; Chand et al., 2009). How the absorbing aerosol ages during transport, thereby affecting the SSA, is not well known, with current surface-based remote sensing characterization limited to the AERONET site at Ascension Island (Satheesh et al. 2009). The comparison of the SSA deduced from the in situ profile of nephelometer measurements shown in Figure 4 to those over mainland Africa would estimate that the SSA increases from 0.84 over mainland Africa, to 0.91 during the weeklong transit to Ascension Island (Haywood et al. 2003). The cumulus clouds most prevalent at Ascension Island are also not realistically modeled by the plane-parallel radiative assumption (e.g., Zuidema et al. 2008).

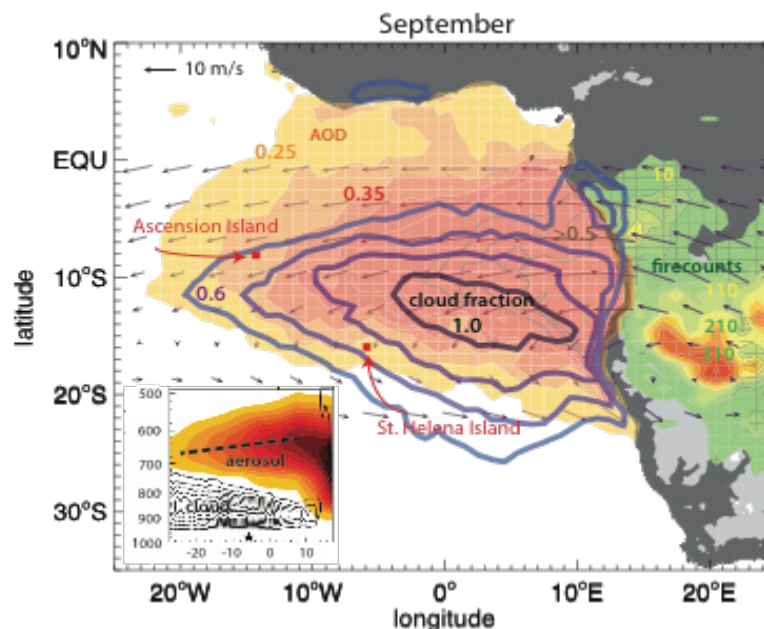


Figure 3. During September, 600 hPa winds escort the BB aerosol (optical depth in warm colors) from fires in continental Africa (green to red, firecounts) westward over the entire south Atlantic stratocumulus deck (cloud fraction in blue contours). The inset, a 4° E to 7° E longitude slice, highlights the main aerosol outflow occurring at 10° S, subsiding to the north where the boundary layer also deepens. The main figure is based on MODIS 2002 to 2012 data and the ERA-Interim Reanalysis; inset on the space-based Cloud Aerosol Lidar with Orthogonal Polarization (CALIOP) and CloudSat 2006 to 2010 data.

Most of the black carbon (BC) emanating from Africa is released by the open burning of grasslands, with incomplete combustion being the norm (Bond et al. 2013). The emissions are thought to be accompanied by large organic aerosol components that also contribute to shortwave and ultra-violet absorption, with

the fractional attribution uncertain. The mass absorption cross-section for BC can thereby increase by approximately 50% as the BC becomes internally mixed with other aerosols. AERONET SSA measurements over land also show a seasonal evolution of SSA from 0.85 to near 0.9 (Eck et al. 2013), attributed to changes in fuel types as the BB shifts further to the south. The change of the net radiative properties of the BB aerosol from July to November is therefore not well understood. The unprecedented sampling throughout the full annual cycle afforded by Layered Atlantic Smoke Interactions with Clouds (LASIC) will answer the question of whether and how the radiative properties of the smoke evolve both offshore and over land.

1.2 Smoke-Cloud Interactions

As the BB aerosol flows out over the Atlantic Ocean, remarkable and poorly understood interactions with the low clouds occur. These interactions depend crucially on the relative vertical location of the BB aerosol relative to the cloud deck. When the smoke is situated directly above the cloud field, the atmospheric stabilization through warming further supports the cloud field, thickening the cloud and increasing the cloud fraction (Johnson et al. 2004). Such a cloud adjustment appears to find observational support in satellite analyses (Loeb and Schuster 2008; Wilcox 2010; 2012; Adebisi et al. 2015). The enhanced cloudiness constitutes a potentially substantial contribution to the net effective radiative forcing that exceeds that from the aerosol alone; it is capable of increasing the surface cooling from $\sim 0.2\text{K}$ to 2K (Sakaeda et al. 2011). An almost unexplored process issue, however, is the mechanism by which atmospheric warming and aerosol scattering that is maximized at the level of maximum aerosol density at $\sim 650\text{ hPa}$ is transmitted to the boundary layer cloud residing $\sim 200\text{ hPa}$ below. The impact of shortwave attenuation by aerosol scattering on the cloudy boundary layer (e.g., by discouraging decoupling within the boundary layer) and the longwave impact of the anomalous moisture present within the aerosol layer (Adebisi et al. 2015) should also be considered.

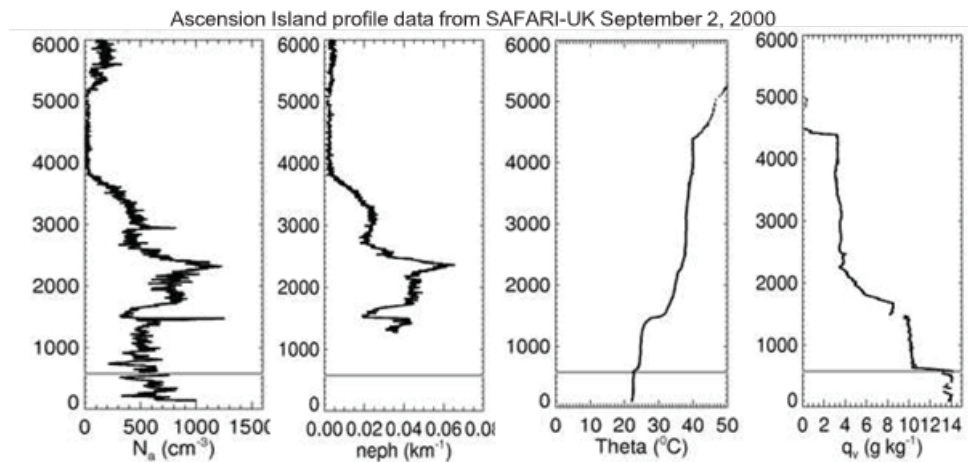


Figure 4. From left to right: vertical profiles of PCASP accumulation-mode aerosol concentration and the nephelometer scattering coefficient at 0.55 micron indicate aerosol concentrations exceeding 500 cm^{-3} in the boundary layer, with the potential temperature and water vapor mixing ratio profiles indicating two well-mixed layers. The grey line indicates cloud base height. Data sampled while descending near Ascension Island on September 2, 2000. Plot courtesy of Steve Abel, U.K. Met Office.

If the BB aerosol is located within the cloudy boundary layer, the shortwave absorption warms the cloud and surrounding atmosphere, lowering the relative humidity and, therefore, the cloudiness (Ackerman et

al. 2000; Johnson et al. 2004; McFarquhar and Wang 2006; Hill and Dobbie 2008; Koch and Del Genio 2010). Biomass-burning aerosols can also become entrained into the clouds themselves. While BC is hydrophobic, other aerosols, particularly organic aerosols, coalesce with the BC during transport and increase its hygroscopicity and therefore its effectiveness as cloud condensation nuclei (CCN). Cloud processes such as nucleation and impact scavenging in turn affect the aerosol mass and provide feedback further into the ability of the aerosol to act as CCN. Results from the SAFARI campaign indeed suggest that CCN number increase in aged BB plumes (Ross et al. 2003). The activated aerosol can then provide a radiative forcing through their reduction of the mean droplet size, while all else held constant (Twomey 1977). There is large-scale evidence of altered microphysics from BB aerosol in the southeast Atlantic from satellite analyses (Constantino and Breon 2010, 2013; Painemal et al. 2014). The activated aerosol can also affect the likelihood of precipitation (e.g., Feingold and Seibert 2009; Wang et al. 2010; Terai et al. 2012). From DOE measurements collected in the Azores, the rain-rate at cloudbase, R_{cb} , is proportional to the liquid water path (LWP) as $LWP^{1.68 \pm 0.05}$ with an assumed supersaturation of 0.55% (Mann et al. 2014). The questions of how these exponents change when absorbing smoke particles become the dominant aerosol type and whether models reproduce these power relationships well are of great interest. In addition, the precipitation susceptibility to the CCN number (N_{CCN}) ranges between 0.5 and 0.9 and generally decreases with LWP (as shown in Figure 5a).

Precipitation susceptibility estimates are not yet known reliably for clouds impacted by long-range BB aerosol transport. Measurements from LASIC will provide an excellent opportunity to enhance analysis and intercomparisons of precipitation susceptibility to other aerosol proxies (such as aerosol optical depth, and aerosol index), and to help resolve outstanding discrepancies among various studies. The dependence of the probability of precipitation (POP) to N_{CCN} (S_{POP}) also varies between observations from ground-based and aircraft deployments (Figure 5b) and satellites and simulations (Figure 5c). S_{POP} from value AMF data is higher than that derived from CloudSat, and is equivalent to that from aircraft observations (Figure 5b) and high-resolution simulations (Figure 5c).

This indicates that the high-resolution, multi-scale climate model may have already had the ability to represent aerosol-cloud-precipitation interactions properly. More experiments such as an intercomparison between high-resolution, ground-based measurements and simulations over other sites for a longer period will provide further valuable confirmation. Ultimately, this focus can be used to improve global models, which at this time significantly overestimate drizzle frequency, thus calling into question the fidelity with which the second indirect effect of aerosol is captured.

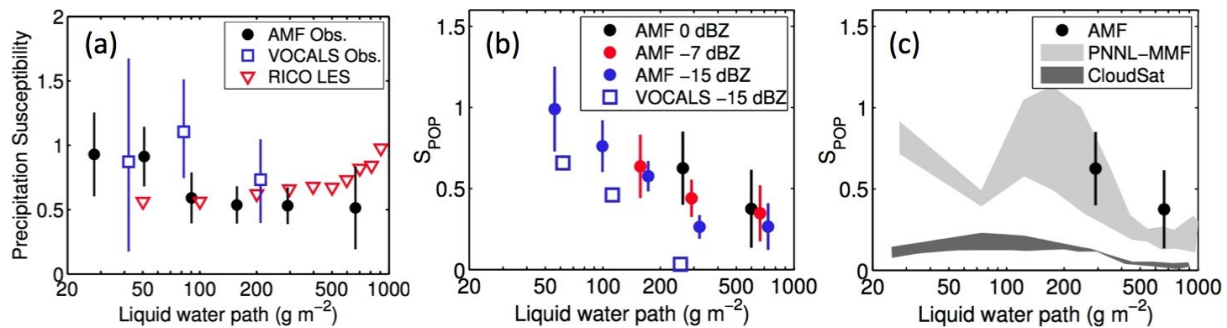


Figure 5. Precipitation susceptibility as a function of LWP in AMF data (with respect to N_{CCN}) and from VAMOS Ocean-Cloud-Atmosphere-Land Study (VOCALS) and RICO large-eddy simulation (LES) data sets (with regard to droplet number concentration [Nd]; Terai et al.

2012; Sorooshian et al. 2009). Susceptibility of POP (S_{POP}) from b) AMF data and VOCALS, and c) CloudSat data and PNNL-MMF outputs at 4-km resolution (Wang et al. 2012).

For BB aerosol, the indirect effects must be compared in relative magnitude against at times opposing semi-direct effects, if, for example, clouds are brightened as their cloud drop sizes decrease, but overall cloud fractions decrease (McFarquhar et al. 2004; Johnson 2005). The recent availability of scanning cloud radars within the DOE mobile deployment pool raises the intriguing possibility that “cloud burn-off” and changes in microphysics can be simultaneously observed as a function of the boundary-layer absorbing aerosol concentration.

2.0 LASIC Activities, Goals, Hypotheses, and Instrument Tables

2.1 Activities

Four activities are proposed for this LASIC campaign: 1) improve current knowledge regarding aging during transport of BB aerosol radiative properties as a function of the seasonal cycle; 2) establish the aerosol-cloud vertical structure; 3) improve our understanding of cloud adjustments to the presence of shortwave-absorbing aerosol within the vertical column, both through aerosol-radiation and aerosol-cloud interactions; and 4) provide observations that will support low-cloud parameterization efforts for climate models. Aerosol-free conditions within the measurements of the full annual cycle provide a reference state, and the mean evolution of smoke properties will be evaluated from July to November. The LASIC campaign consists of a deployment of AMF1 instrumentation (the Mobile Aerosol Observing System and ground-based remote sensors) from June 1, 2016 until October 31, 2017 (see Table 1 for a complete list of instrumentation). An intensive operational period (IOP) consisting of 8x/daily radiosondes for two months is scheduled to coincide with the U.K. and NASA aircraft deployments (detailed further below) and with the highest aerosol loading occurring from August 1-September 31, 2016. This characterization of the diurnal cycle of the boundary-layer thermodynamic and kinematic vertical structure is unprecedented for the southeast Atlantic Ocean. This characterization will be maintained at 4x/daily radiosondes during the rest of the deployment.

2.2 Goals

The scientific goals of the LASIC campaign are articulated through the following hypotheses:

- Hypothesis 1 (H1)** The SSA of the carbonaceous aerosol overlying Ascension Island increases during the BB season as has been documented over land.
- Hypothesis 2 (H2)** Low-cloud properties at Ascension Island vary as a function of the amount, vertical distribution, and optical properties of absorbing aerosol aloft that is distinct from meteorology.
- Hypothesis 3 (H3)** Carbonaceous aerosol are present within the Ascension Island boundary layer, where they are capable of affecting cloud microphysics, precipitation susceptibility, and cloud mesoscale organization.

Hypothesis 4 (H4) The evolution of the cloudy boundary layer between St. Helena Island and Ascension Island varies as a function of the absorbing aerosol loadings aloft and large-scale environmental parameters such as sea-surface temperature.

The science goals and objectives of the campaign will be achieved by:

1. Characterizing the microphysical and optical properties of the carbonaceous aerosol at Ascension Island as a function of time.
2. Characterizing the low-cloud properties at Ascension Island as a function of the vertical location and optical properties of the absorbing aerosol within the atmospheric column, controlled for thermodynamic state and prior cloud evolution.
3. Assessing the aerosol size distribution and hygroscopicity and relating the aerosol properties to the cloud spatial distribution, its microphysics, precipitation susceptibility, and cloud mesoscale organization when carbonaceous aerosol is present within the boundary layer.
4. Assessing the evolution of the cloudy boundary layer from St. Helena to Ascension Island under a wide range of atmospheric aerosol conditions as well as large-scale environmental conditions.

2.3 Instrumentation

Table 1 lists the specific AMF1 instrumentation requests for deployments from Ascension Island. These include the MAOS-Aerosol and MAOS-Chemistry (MAOS-A and MAOS-C) packages, which will be relocated from the GoAmazon deployment in Brazil to Ascension Island via the US, providing an opportunity to maintain and calibrate the instruments. Priority instruments, at this point, are identified with asterisks. Table 2 lists the U.K. Met Office/UMiami instrumentation anticipated for St. Helena as part of the Cloud-Aerosol-Radiation Interactions and Forcing (CLARIFY) campaign. Further planning details, including additional anticipated and desired instrumentation and campaign-specific priorities including value-added products (VAPs), are discussed in Section 4.0.

Table 1. AMF1 Instrumentation

MAOS Baseline Instrument	Function
MAOS-Aerosol (MAOS-A)	
Sonic Detection and Ranging (SODAR) System	wind velocity in the lower atmosphere
Ultra-High-Sensitivity Aerosol Spectrometer (UHSAS)*	aerosol size and number, 50 nm-1micron
Dual-Column CCN Counter*	# of activated aerosols at 2 supersaturations
Single-Particle Soot Photometer (SP2)*	black carbon mass and size
Scanning Mobility Particle Sizer (SMPS)*	aerosol size distribution, 15-450 nm
Photo-Acoustic Soot Spectrometer (PASS)*	aerosol absorption and scattering coefficient at 3 wavelengths
Humidigraph (scanning RH w/ 3 single-wavelength nephelometers)*	aerosol scattering coefficient as a function of relative humidity

MAOS Baseline Instrument	Function
Nephelometer, 3-wavelength*	aerosol scattering coefficient
Condensation Particle Counter (CPC)*	condensation particle concentration, 10 nm->3000 nm particle size
Condensation Particle Counter (CPC2)*	condensation particle concentration, 2.5 nm->3000 nm particle size
Hygroscopic Tandem Differential Mobility Analyzer (HTDMA)*	aerosol growth factor as function of humidity
Particle Soot Absorption Photometer (PSAP)*	aerosol extinction/absorption (black carbon)
7-wavelength Aethelometer (AETH)*	aerosol extinction/absorption (black carbon)
Weather Transmitter (WXT-520)*	T, RH, u, v, rainfall, p
Aerosol Chemistry Speciation Monitor (ACSM)*	aerosol mass and composition
MAOS-Chemistry (MAOS-C)	
Trace Gas Instrument System*	CO, SO ₂ , NO/NO ₂ /NO _y , O ₃
Proton Transfer Mass Spectrometer (PTRMS)*	volatile organic compounds
AMF1	
3-channel Microwave Radiometer (MWR3C)*	integrated liquid water and water vapor
Balloon-borne Sounding System (SONDE)* 4x/daily increasing to 8x/daily for 2 months	temperature, humidity and wind vertical structure
Ceilometer (VCEIL)*	cloud base
Radar Wind Profiler (RWP)*	wind vertical structure
W-band Scanning Cloud Radar (WSACR)*	cloud and precipitation spatial structure
W-band Zenith Cloud Radar (WACR)*	cloud and precipitation vertical structure
K-band Scanning Cloud Radar (KASACR)*	cloud and precipitation spatial structure
Micropulse Lidar (MPL)*	aerosol vertical structure
Atmospheric Emitted Radiance Interferometer (AERI)*	cloud liquid water path and effective radii
Multifilter Rotating Shadowband Radiometer (MFRSR)*	aerosol optical depth
Narrow Field of View (NFOV)*	cloud optical depth and effective radius
Solar Array Spectrometer (SASHE & SASZE)*	radiative closure
Surface Energy Balance System (SEBS)*	surface energy balance. soil moisture and flux measurements are not needed
Surface Radiation Measurements (SKYRAD, MFR, GNDRAD)*	surface radiation balance (overlap with SEBS?)
Meteorological Instrumentation (MET)*	surface air layer properties
Optical Rain Gauge (ORG)*	surface rain
Parsivel Disdrometer	rain drop size distribution
Tower Camera (TWRCAM)*	photo imagery
Total-Sky Camera (TSI)*	cloud fraction
Doppler Lidar (DL)	clear-sky vertical velocities
Ka-band ARM Zenith Radar (KAZR); additional instrument for LASIC only	cloud and precipitation vertical structure

3.0 Specific Objectives

3.1 Characterizing Aged Carbonaceous Aerosol (H1)

Most BB aerosol measurements are taken close to their source. Yet, the carbonaceous aerosol that alter the radiative fluxes and heating rates over the Atlantic Ocean are already aged by at least a day, with the transport time to Ascension Island taking five to six days (Adebisi et al. 2015). In situ characterization during SAFARI-2000 concluded that most of the aerosol aging occurs within the first few hours after leaving the source region (Abel et al. 2003), with the SSA rising by 5% over that time. Vakkari et al. (2014) similarly found that atmospheric oxidation and subsequent secondary aerosol formation drive large changes in BB aerosol properties in the first two to four hours of transport. However, a satellite-based study suggests BB aerosol sizes and therefore the SSA continue to evolve during aerosol transport over the Atlantic (Waquet et al. 2013). Ascension Island is 3000 km from the African coast, so the comprehensive surface-based aerosol measurements possible with the Mobile Aerosol Observing system will assess the properties of the truly aged aerosol. Because the characterization is occurring so far from the BB source, these surface-based aerosol characterizations can be considered representative of the carbonaceous aerosol properties throughout the vertical column. These surface-based measurements will characterize those properties of BB aerosols most needed to model the direct radiative forcing—the mass absorption and scattering cross-sections and mass concentrations. Measurements specifically aimed at characterizing the aerosol SSA include the photo-acoustic soot spectrometer (PASS), the particle soot absorption photometer (PSAP), the seven-wavelength aethelometer, and the humidigraph. The humidigraph is able to assess the aerosol scattering coefficient using three different wavelength nephelometers as a function of relative humidity.

Closure studies will link absorption to measurements of BC mass and mixing state, such as from the single-particle soot photometer and aerosol chemistry speciation monitor (ACSM). Column radiative closure studies with the multifilter rotating shadowband radiometer (MFRSR) and SAS-Ze on cloud-free days, alone or in combination with aerosol vertical profile information from the micropulse lidar (MPL) (see Section 3.3), will characterize the column-average aerosol properties needed to match the observed surface radiance and thus provide information on the aerosol aloft. This work goes hand in hand with developing retrievals for the SAS-Ze and SAS-He spectral radiometers. The LASIC observations will provide an independent opportunity to evaluate the ARM 3-wavelength aerosol best estimate (ABE) VAP. This will be done by comparing calculations from the LBLRTM/CHARTS radiative transfer model (Mlawer et al. 2000) using the ABE profiles as inputs to the observations of the SAS-Ze and SAS-He spectral radiometers near the ABE reference wavelengths. The SAS-Ze and SAS-He measurements will lend themselves to better estimates of aerosol optical depth (AOD), SSA, and asymmetry parameter (g). Because these properties are determined mostly by the aerosol composition and size distribution, the strategy is to determine the column-integrated aerosol size distribution and complex index of refraction (which is a function of aerosol composition) that is most consistent with the available SAS-Ze and SAS-He data, similar to the method of Kassianov et al. (2007) for the ARM MFRSR. Further colocated measurements of aerosol chemical composition, size distribution, and optical properties, along with knowledge of sources and air transport, will be evaluated in relation to column and profile properties from ground-based passive and active remote sensors, thereby providing a fuller and more accurate characterization of the aerosol throughout the column.

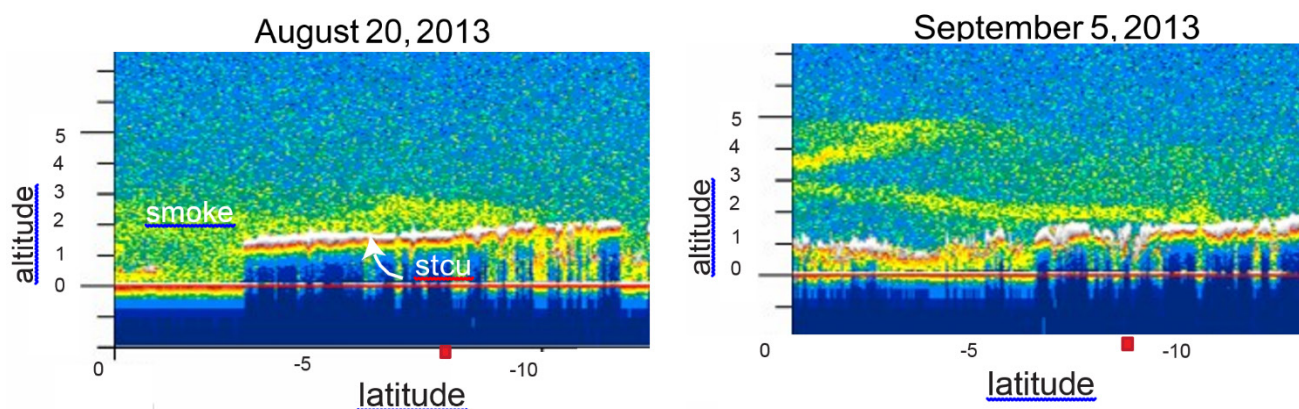


Figure 6. CALIOP snapshots of 532-micron backscattered intensity near Ascension Island suggest a range of cloud-aerosol interactions. The latitudinal location is indicated as a red box on x-axis.

Further measurements will assess the ability of the aerosol to act as a CCN, with an ultra-high sensitivity aerosol spectrometer (UHSAS) as well as a scanning mobility particle sizer (SMPS) providing the sizing over the dominant condensation nucleation size ranges (50 to 1000 nm and 15 nm to 450 nm, respectively). Such data sets will be combined with a dual-column CCN counter capable of counting the number of aerosols activated into CCN at two representative and independently selected supersaturation levels. Such measurements are integral to providing constraints for aerosol-cloud modeling, including for the AeroCom project. In addition, efforts will be made to analyze the chemistry of the carbonaceous aerosol. This will be done using the updated Aerosol Simulation Program, with updated gas-phase chemistry and the Volatility Basis Set (VBS) scheme for SOA formation (Alvarado and Prinn 2008; Alvarado et al. 2015). This improved version has been used to analyze the chemistry of a South Africa savannah fire smoke plume (Hobbs et al. 2003) and the Williams fire smoke plume sampled by Akagi et al. (2012).

3.2 Accurate Identification of Aerosol-Cloud Vertical Structure (supports H2, H3 and H4)

The vertical distribution of the absorbing aerosol and low cloud and their spatial and temporal variability must be known before radiative forcings and cloud adjustments can be adequately characterized. The importance of an accurate characterization, and our current lack of one, is worth emphasizing. Space-based lidar is currently our best source of information (e.g., Figure 6). From space, the optically thin aerosol layer base must be detected after the lidar signal is attenuated by the intervening aerosol. During the day, vertical sampling is hindered by solar interference so that retrieved daytime smoke base altitudes are placed 500 m higher in the mean compared to nighttime altitudes (Meyer et al. 2013). Thus, CALIOP cloud-aerosol separation statistics tend to suggest little cloud-aerosol overlap and therefore little aerosol entrainment into the cloudy boundary layer (Meyer et al. 2013). However, this is contradicted by satellite studies of the clouds themselves (e.g., Constantino and Breon 2013; Painemal et al. 2015), and anecdotally by the available in situ data such as shown in Figure 4.

A definitive climatology of how often free-tropospheric aerosols interact with clouds rooted within the boundary layer requires long-term, high time resolution, surface-based lidars and radars. These instruments provide much more detailed and vertically resolved profiles of aerosol and clouds than is

possible from space. The aerosol vertical structure statistics also further our understanding of the transport and eventual deposition patterns of BB aerosol. The AMF1 Micropulse Cloud Lidar (MPL) will be able to resolve the vertical structure to 30 m. Ascension Island is already an AERONET site, and the DOE MPL data set can potentially contribute constructively to a merged data set with the AERONET data. This will require coordination with MPLNET protocols (Welton et al. 2001). The surface-based W-band Zenith Radar (WACR) primarily, and the scanning Ka-band and W-band cloud radars (KASACR and WSACR), provide an accurate view of the cloud and precipitation vertical structure, resolved to 50 m, that will then be integrated with the lidar-derived aerosol statistics.

3.3 Cloud Adjustments to Aerosol-Radiation and Aerosol-Cloud Interactions (H2, H3)

If the surface-based aerosol measurements and vertically profiling lidar indicate that BB aerosol is present within the cloudy boundary layer, the DOE measurements will support scientific inquiry into the resulting cloud adjustments. These include what has colloquially been referred to as the “cloud burn-off” effect, whereby shortwave absorption by the aerosol increases the local temperature, thus decreasing the relative humidity and discouraging cloud growth. If this effect is also induced by BB aerosols entrained into boundary-layer cloud drops, a reduction in the mean drop size can occur for the same liquid water content, potentially reducing precipitation or enhancing evaporation even further. To date, the impact of entrained BB aerosol in the boundary layer has been examined for INDOEX data (Ackerman et al. 2000) and the Amazon (e.g., Feingold et al. 2005). In both field experiments, the smoke was already present within the boundary layer.

The hyper spectral irradiance and radiance measurements from the scanning spectral solar array spectrometer-hemispheric and -zenith (SASHE and SASZE) radiometers in the visible and near-infrared (NIR) regions will be applied to help separate the respective aerosol-cloud signatures. The NIR wavelengths are able to reveal a much finer cloud structure than the visible wavelengths, mainly because the higher NIR-absorption by liquid water reduces the radiative smoothing effect of cloud multiple scattering. The better knowledge of cloud properties from the NIR wavelengths can then improve the characterization of aerosol optical properties towards achieving radiation closure.

Such measurements, when combined with the dual-wavelength scanning Ka-band and W-band cloud radars (KASACR and WSACR) and with longer-term instruments possessing well-characterized retrieval algorithms, such as the MFRSR, microwave radiometer profiler, and a 3-channel and high-frequency microwave radiometer (MWR3C and MWRHF), are well-poised to provide insight into the relative magnitude of radiative effects from aerosols and clouds. The net radiative impact will be succinctly summarized by the downwelling radiation (SKYRAD) and SEBS measurements, and surface-based rain gauges will assess how much precipitation reaches the surface and leaves the atmosphere. Precipitation susceptibility estimates can then be generated using the WACR-derived precipitation estimates, microwave-derived LWP, the CCN counter-concentration values, and other aerosol proxies.

As noted previously, such susceptibility metrics have been found to systematically differ from those derived using space-based remote sensing at larger scales (Figure 5), with implications for how these metrics are used to parameterize climate models. The long-term statistics from Ascension Island, occurring within a different aerosol-cloud regime, will provide an opportunity to test the universality of

these results. These observational efforts will be coordinated with high-resolution modeling of aerosol-cloud processes.

The precipitation particle size distributions from the Parsivel disdrometer and the optical rain gauge rainfall rate measurements will furthermore be used to adjust (i.e., calibrate) the radar wind profiler (RWP) power measurements using the techniques developed by Tridon et al. (2013). Using the newly proposed RWP operational modes, we will have cloud and precipitation observations from the surface throughout the full depth of the atmosphere with no attenuation. Combining the RWP with the WACR observations will provide a dual-wavelength view of clouds and precipitation. The RWP will also contiguously map the inversion height (compared to the four to eight daily measurements from the soundings) and help identify the entrainment episodes of free-tropospheric air that are so critical for bringing smoky free-tropospheric air into the boundary layer.

The Ka/W-scanning ARM cloud radars (Kollias et al. 2014a) will provide information on the mesoscale structure and organization of the cloud fields (Kollias et al. 2014b), including on the horizontal wind fields in the cloud layer. The Ka/W-SACR will be used to track cloud structures and study the lifetime of isolated cumuli clouds (Borque and Giangrande et al. 2014). The recorded radar Doppler spectra can be used to assess the early drizzle growth (Kollias et al. 2011a; 2011b) as a function of variable aerosol conditions. From the constructed three-dimensional cloud structure (Lamer et al. 2013), the vertical velocity field can be retrieved and applied to entrainment studies using the profiling and scanning cloud radar observations.

When the absorbing aerosol layer is entirely located above the cloud, stabilization of the atmosphere at that level may encourage cloudiness by discouraging the entrainment of warmer, drier air into the boundary layer. The absorbing aerosol layer aloft is typically associated with anomalous moisture (Adebiyi et al. 2015), aiding hygroscopic growth of the aerosol that further increases its ability to scatter shortwave radiation. The moisture-swelled aerosol attenuates the shortwave radiation reaching the cloud, while the longwave opacity of the moisture will diminish the cloud-top longwave cooling. If all else is equal, solar-induced decoupling should be reduced within the boundary layer when absorbing aerosol is present overhead, fostering a more well-mixed boundary layer. On the other hand, the reduced cloud-top, longwave cooling will drive less turbulence within the boundary layer, providing the opposite feedback. Thus, the inference of cloudy boundary-layer adjustments to free-tropospheric aerosol loadings will require knowledge of the boundary-layer decoupling. The balloon-borne sounding system (SONDE) data sets will be applied to assess boundary-layer decoupling throughout the annual cycle.

WACR radar data will help distinguish the impact of turbulent mixing from microphysics on the spectrum width (e.g., Fang et al. 2012). The evolution of the boundary layer can also be characterized using a new AERI-based retrieval that is able to infer temperature and humidity profiles at high time resolution from both clear and cloudy sky sciences (Turner and Loehnert 2014).

A vertical profile of aerosol extinction can be inferred from the lidar backscattered intensity using AERONET or other aerosol optical depths as a constraint. The SSA will be determined from the surface aerosol measurements and assumed to represent the entire column. The cloud optical depth can be inferred from NFOV or sun photometer zenith radiance measurements (Chiu et al. 2012). From these inputs, estimates of the aerosol heating rates can then be calculated. When clouds are inhomogeneous, radiative transfer results can be filtered for spectrally consistent data that can be compared to SASZE and

SASHE measurements, similar to what has been done with an aircraft-based solar spectral flux radiometer (Kindel et al. 2011).

When the aerosols are embedded within the cloud layer, a similar statistical combination of modeling and measurements can quantify the heating rates (Schmidt et al. 2009). Competing radiative impacts from changes in microphysics and cloud spatial organization can be discriminated using three-dimensional radiative transfer modeling of large-eddy simulations initialized by the observations and compared to measured irradiances (Zuidema et al. 2008; Schmidt et al. 2009).

Such radiative closure provides a means of not only assessing retrieval accuracy, but also for extrapolating local observations with confidence to larger scales. This represents a significant opportunity for satellite retrieval development and assessment within a difficult space-based remote sensing regime.

3.4 Distinguishing Aerosol from Meteorological Effects (H2, H4)

A first-order activity is to understand the depth and complexity of the well-coupled aerosol-meteorological state. It is imperative that the meteorology be well-characterized, toward constraining modeling simulations and confidently distinguishing aerosol effects. As much of this work as possible will be done prior to the campaign. Burning over continental Africa occurs throughout the year, but the circulation pattern that favors westward advection during the aerosol occurs primarily between July and November, and is most pronounced in September and October. During that period, the aerosol-bearing southerly African easterly jet (Jackson et al. 2009), centered at approximately 10° S, or near the latitude of Ascension Island, is most pronounced (Adebiyi et al. 2015). This outflow is accompanied by moisture that also influences the cloudy boundary layer. Boundary-layer clouds are known to be highly influenced by boundary-layer conditions prevailing 24 to 36 hours upstream (e.g., Klein et al. 1997; Mauger and Norris 2007), which for Ascension Island occurs southeast of the island. Thus, unlike the southeastern Pacific, a strong wind shear exists between the free-tropospheric and boundary-layer winds (compare, e.g., Figure 1 with Figure 3).

The meteorological conditions encouraging aerosol outflow and their dynamical impact on the low-cloud fields will be characterized using daily ERA-Interim Reanalyses (e.g., Adebiyi et al. 2015), with the goal of defining an easy-to-apply meteorological metric associated with the aerosol outflow (e.g., the strength of the southerly African Easterly Jet, Adebiyi et al. 2016). Thermodynamic observations of the entire annual cycle (Figure 7) confirm that large-scale conditions at Ascension Island are consistently representative of the trade-wind conditions, easing the ability to identify smoky and pristine large-scale conditions with similar thermodynamic context at Ascension. The natural variability of the low-cloud fields at Ascension will be examined using satellite data as a function of both the aerosol-associated meteorological metric and the cloud upwind conditions as defined by ERA-Interim Reanalysis data sets prior to the campaign. The four-times-daily soundings, increasing to eight-times daily during the August through September IOP, combined with an RWP, will characterize Ascension Island's wind vertical profile and can help fine-tune the analysis begun with ERA-Interim data sets. U.K. Met Office measurements at St. Helena Island, which is upstream of Ascension Island if considering the boundary-layer winds but downstream if considering the free-tropospheric winds driving the aerosol outflow, will be related to the DOE measurements at Ascension Island.

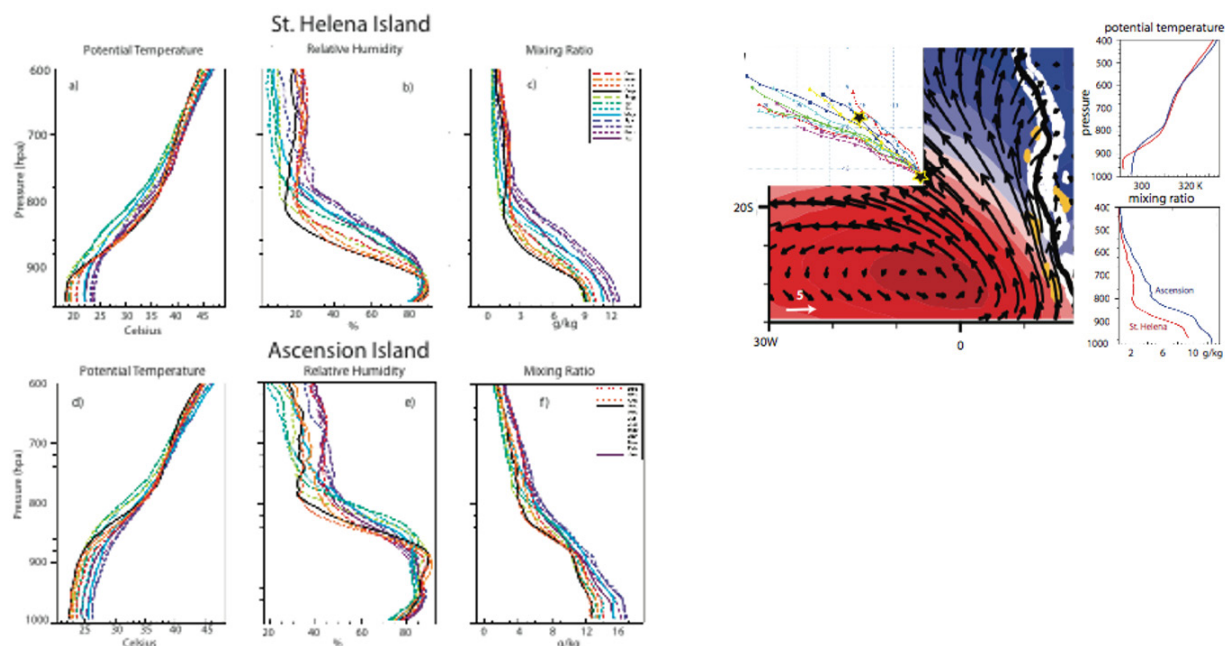


Figure 7a-g. Monthly-mean profiles of atmospheric potential temperature, relative humidity, and mixing ratio clearly highlight the warmer, deeper, and more moist boundary layer at Ascension Island (bottom row) compared to St. Helena Island (top row), and the distinct seasonal cycle at each location from 2000 to 2012 Integrated Global Radiosonde Archive soundings (radiosondes were discontinued at Ascension Island after 2012). Right panel: September through October ERA-Interim 1000 hPa climatological winds and sea-level pressure with an ensemble of September 2013 HYSPLIT forward trajectories from St. Helena Island (superimposed) passing near Ascension Island, and September-mean thermodynamic profiles from both islands.

At smaller scales, a new data set of high-frequency cloud-fraction observations based on merged geostationary infrared data will be applied to investigate the joint variability of meteorological and cloud properties, as has been done over the Azores region (SE Yuter, personal communication). These techniques will explore cloud and precipitation properties along the transition from the stratocumulus boundary to the trade cumulus regime for the southeast Atlantic. A synoptic classification scheme, developed from a combination of reanalysis and MODIS observations, will be used to characterize the boundary layer and cloud properties using ARM observations. The relationship between inversion strength and low-cloud properties as a function of time scale will also be evaluated by correlating International Satellite Cloud Climatology Project-derived cloud properties and synoptic state from National Centers for Environmental Prediction reanalysis.

Simulations using models of varying complexity and resolutions will subsequently and independently quantify the influence of aerosol through simulations with and without aerosols (e.g., Sakaeda et al. 2011). These simulations will be constrained by the DOE-measured vertical profiles of temperature, moisture, and winds as well as from reanalyses, using both aerosol-free and aerosol-contaminated conditions to help distinguish the various contributions. Idealized simulations representing the range of observed conditions will also help articulate and quantify the range of adjustments possible. Another approach will combine Weather Research and Forecasting (WRF) meteorological fields with a Lagrangian particle dispersion model (FLEXPART-WRF) to calculate trajectories and estimate concentrations of tracers within the WRF domain (Brioude et al. 2013). Those tracers will correspond to

point sources of southern African fires and other terrestrial sources that might impact the aerosol burden in the region of interest. FLEXPART-WRF uses MODIS-derived fire data to estimate BB source functions and injection heights for the simulation of the transport pathways of the BB plumes. The tracers are passive, but wet deposition parameterizations based on meteorological fields from WRF can be applied and tested.

3.5 Measurements that Span the Full Annual Cycle, and Low-Cloud Model Parameterization Development Support (H2, H4)

The BB aerosol radiative properties will be evaluated at Ascension Island as a function of time during the July through November BB-burning season. Should the smoke SSA be determined to trend systematically at remote Ascension Island, this will also impact the radiative-heating profile. The impact (and frequency) of BB aerosol entrained into the boundary layer may in turn also evolve with time, and will be evaluated. AERONET measurements from the continent and at St. Helena Island will help determine if and how similar systematic trends typify all of the locations.

The seasonal cycle is also an important metric with which to assess the behavior of low clouds within climate models. Many CMIP5 models exhibit a seasonal cycle in the liquid water path that is out of phase with the observed seasonal cycle over the main stratocumulus deck (Figure 8) as defined within Klein and Hartmann (1993; 10° to 20° S, 0° to 10° E). Modeled skill at capturing the annual variation in low-cloud fraction has been shown to increase for models with more realistic annual cycles in the lower tropospheric stability (Noda and Satoh 2014), suggesting that the problem lies more with the internal cloud parameterizations than with the climate model depictions of the large-scale state. Ascension and St. Helena Islands can serve as foci for more detailed output of the next-generation CMIP6 models to further diagnose model behavior.

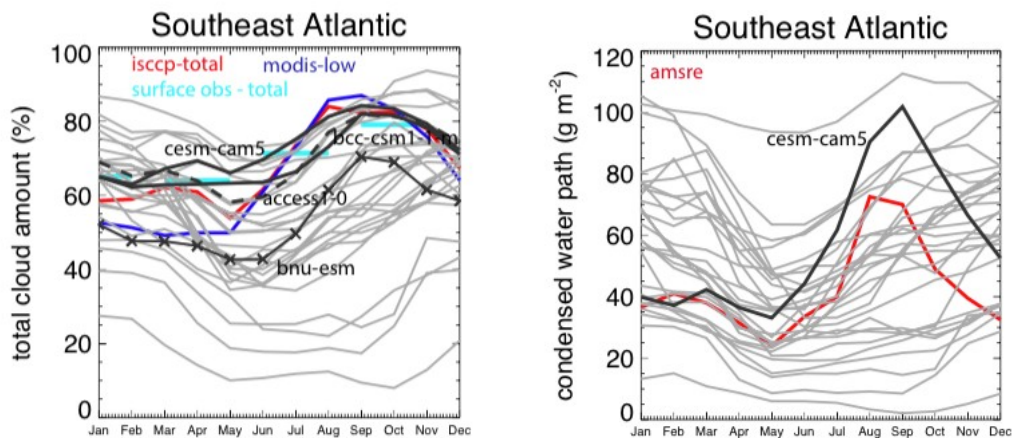


Figure 8. The annual cycle in (left) cloud amount and (right) LWP over the 10° to 20° S, 0° to 10° E region (Klein and Hartmann, 1993) in CMIP5 models and observations. These include the International Satellite Cloud Climatology Project, Extended Edited Cloud Report Archive, and MODIS and AMSR-E (2002 to 2012). The black lines indicate CMIP5 models with the highest correlations to the observed values. The DOE-supported CESM-CAM5 model depicts the most realistic annual cycle of the models shown supporting further cloud parameterization activities.

A correct seasonal cycle in cloud fraction and cloud properties in both global aerosol models and climate models lacking aerosol representation is a prerequisite for models seeking to further improve the internal cloud model representation. The concurrent radiosonde thermodynamic profiles combined with cloud property measurements will allow for a sensitive interrogation using a range of models, from process-level, large-eddy simulations, to climate models, for further parameterization efforts for low clouds. Efforts will be made to advance modeling foci on low clouds by ensuring and developing the VAPs most useful for Climate Process Teams, the DOE Cloud-Associated Parameterizations Testbed, the DOE Aerosol Modeling Testbed, and the Large-Eddy Simulation Testbed. The radiosondes, most particularly during the IOP when radiosondes are launched 8x/day on Ascension Island, along with more radiosondes launched on St. Helena by the U.K. Met Office, will provide crucial initialization and evaluation products.

4.0 Site Description, Planning, Value-Added Products, and Collaborations

4.1 Site Description

Ascension Island is governed as part of a larger British Overseas Territory that includes St. Helena Island and Tristan da Cunha. The island does not maintain a permanent population, and a contract of employment is required for residence upon the island, although opportunities for tourism are becoming more available. The U.K. Royal Air Force and U.S. Air Force both maintain a presence, centered on WideAwake Airfield. The US Air Force presence (~20 personnel) is an auxiliary base of Patrick Air Force Base in Florida, and the island is serviced regularly every 60 days by a U.S. cargo ship, the MV Ascension, making round trips to and from Port Canaveral, Florida.

The island has a history of scientific endeavors because of its unique location. It is used as a rocket tracking station, Anglo-American signals intelligence facility, and a BBC World Service relay station. Ground antenna that assist in the operation of the Global Positioning System are installed there as well. Radiosondes were launched from Ascension Island with U.S. government funding until 2012, but no radiosonde launchings have occurred since then. Ascension Island is still an AERONET site. The U.K. Met Office has used Ascension Island as a stop on its ferry flights to and from Africa (e.g., SAFARI), and some limited in situ data are available from those flights (Figure 4). On St. Helena Island, the U.K. Met Office has been launching almost daily radiosondes for many decades, archived at higher vertical resolution since 2000. The higher vertical resolution is a necessary condition for supporting research into aerosol-cloud-meteorological characterization at St. Helena (Adebiyi et al. 2015). Lower-resolution radiosonde data are available for both sites through the Integrated Global Radiosonde Archive database (Figure 7).

Ascension and St. Helena Islands are volcanic remnants with maximum altitudes of 859 and 818 m, respectively. Ascension Island does not intrude above the boundary layer (Figure 9), but the island is nevertheless capable of modifying the flow, primarily visible through a wake effect seen in satellite imagery. This should not affect the surface-based aerosol measurements of mass, composition, and absorption, but the boundary-layer flow modification could affect other parameters such as the mean cloud fraction and cloud diurnal cycle. The island impact on cloudiness will need to be assessed. The total-sky camera will assess local gradients in the cloud cover. A larger-range option for assessing island effects could be through unmanned aerial vehicles (perhaps through DOE's guest instrumentation

program), and to compare aircraft launches and departures to the radiosondes. A satellite approach would be to assess cloud retrievals from the Visible Infrared Imaging Radiometer Suite, available at 750-m resolution at regular times, combined with cloud retrievals from the diurnally resolving geostationary spinning enhanced visible and infrared imager instrument. None of these approaches is optimal, and this will require more thought and discussion, perhaps through evaluating what has been done at other ARM island sites.



Figure 9. Views of Ascension Island. Top: Looking from the northwest, approaching Clarence Bay. Bottom: Looking offshore to the southeast from the AMF1/MAOS site with a 120-degree field of view.

The anticipated distribution of instrumentation on St. Helena is indicated in Figure 10 along with the view from the AMF1 site to the southeast. The AMF1/MAOS will be located at 365 m altitude on the windward side. Its distance from the airport and from other habitation is intended to secure aerosol measurements typical of offshore. The necessary power generator will be located as far away, upwind, from the instruments as possible. The radiosondes will be launched from the airport, adding to a previous long time series. A microwave radiometer will also be placed there, augmenting an existing ceilometer and an AERONET site.

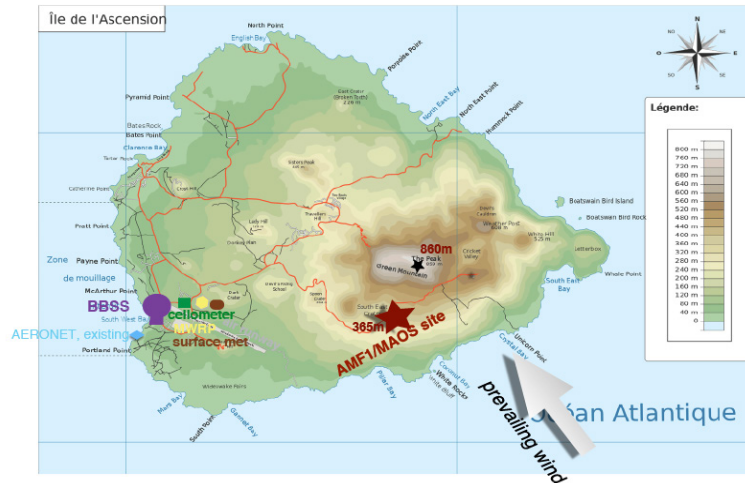


Figure 10. Ascension Island layout of instrumentation.

4.2 Related Campaigns

Complementary activities will be conducted by the U.K. Met Office and NASA. The U.K. Met Office CLARIFY Campaign (PI: Jim Haywood; 2016) deployment of its FAAM BAe-146 plane spans August 21 to September 16, 2016. It will be based in Walvis Bay, Namibia, with a day planned during the transit leg to Namibia to do in situ sampling at Ascension and St. Helena. At St. Helena island, the U.K. Met Office already releases almost-daily radiosondes and operates a ceilometer. The U.K. Met Office will complement these measurements by a suite of surface-based remote sensors for the fall of 2016, as listed in Table 2. The ARM Facility will also support the deployment of the University of Miami W-band Doppler radar to St. Helena. The NASA Observations of Aerosols above Clouds and their Interactions (ORACLES) is a multi-year, multi-aircraft deployment, also based initially at Walvis Bay, Namibia, led by PI Jens Redemann, NASA AMES, and Deputy PI Rob Wood. ORACLES plans to deploy the P-3 and ER-2 planes in 2016, overlapping with CLARIFY. A separate NASA initiative will also be establishing a new AERONET site on St. Helena.

CLARIFY will similarly investigate the direct, semi-direct, and indirect effects of biomass burning aerosols over the SE Atlantic. CLARIFY will focus on using its measurements to immediately improve the U.K. Met Office model, which has incorporated the GLOMAP-mode state-of-the-science aerosol model (Mann et al. 2010; Bellouin et al. 2013). The U.K. suite of remote sensors will provide the upwind (boundary-layer) and downwind (free-tropospheric) information on the evolution of cloud and aerosol properties that are also being sampled at Ascension. These measurements will span from mid-July through October. The U.K. FAAM BAe-146 plane will spend one day on in situ sampling near the Ascension and St. Helena sites on its ferry flight to Namibia. The lead investigator, Dr. Jim Haywood, a co-investigator on LASIC, will facilitate coordination and data sharing between the projects. The unified U.K. Met Office operational forecast model will be applied at 4km resolution for the campaign, with the forecasts shared between all campaigns. Post-campaign modeling exercises are anticipated to incorporate the data sets from all campaigns. Meteorological forecasts done in the context of CLARIFY will be tested with LASIC data sets.

Table 2. U.K. Met Office/UMiami/NASA Instrumentation upon St. Helena, fall 2016 only.

Doppler lidar (U.K. Met Office)	winds
Microwave Radiometer (U.K. Met Office)	cloud liquid water path and water vapor path
Wband Zenith Doppler Cloud Radar (UMiami)	cloud and precipitation vertical structure
Solar and Infrared Broadband Radiometers (U.K. Met Office)	surface broadband fluxes
Radiosondes (U.K. Met Office)	temperature, moisture, winds profiles
Grimm Spectrometer (U.K. Met Office)	optical particle counting
Sun Photometers (NASA, AERONET)	aerosol optical depth

The NASA-ORACLES deployment will overlap with the 2016 LASIC IOP and the CLARIFY-2016 campaigns, during which the NASA P-3 and ER-2 planes will also be based at Walvis Bay, Namibia. The NASA P-3 plane will host aerosol and cloud in situ instrumentation, including a high-spectral-resolution lidar (HSRL-2), cloud radars, and solar spectral flux radiometers. The ER-2 will host airborne remote-sensing tools (another HSRL-2, enhanced MODIS airborne simulator, airborne multiangle spectropolarimeter imager, and a solar spectral flux radiometer) that are important for improving space-based retrievals and to future NASA satellite missions. CLARIFY research flights will take place closer to the Namibian coast, while the longer-range ORACLES flights will still predominantly occur southeast of Ascension, both upstream (boundary-layer) and downstream (free-troposphere) of the airflow encountering Ascension Island. ORACLES includes both survey flights along regular latitude-longitude lines and flights more specifically focused on assessing aerosol direct radiative effect under conditions of varying cloud cover, evaluating the impact of solar absorption by the BB aerosol on the atmospheric stability, and aerosol-cloud microphysical interactions. In its three campaigns between 2016 and 2018, ORACLES will study intraseasonal variations (August to October) in aerosol and cloud properties and their interaction.

A larger scientific coordination group composed of the PIs and other personnel will optimize the coordination between the different campaigns.

Discussions of other possibly complementary science projects follow. At this point, the NASA Atmospheric Tomography Mission (PI: Steve Wofsy, Harvard University) is planning four around-the-world research flights in the next 5 years with stops in Ascension Island to understand the chemical processes controlling methane and ozone. A ground station of the Total Carbon Column Observing Network measures all the major greenhouse gases, described at https://tccon-wiki-caltech.edu/Sites/Ascension_Island (PI: Dietrich Feist, MPI-Biogeochemistry). Unmanned aerial vehicles have been used to measure methane as well (PIs: John Pyle, University of Cambridge and Jim Freer, University of Bristol) and future measurements may coincide with LASIC.

4.3 Priority Value-Added Products and Guest Instrumentation

Development of an ABE VAP that includes an MPL extinction profile will be both a science and a programming priority for LASIC. The MPL does not measure extinction directly. Instead, the back-scattered intensities can be constrained using the AERONET aerosol optical depth to develop an

extinction profile (i.e., to be compatible with MPLNET; other aerosol optical depths can also provide the constraint). Additional aerosol lidars deployed as guest instruments are highly desirable both to ensure redundancy in the measurement and, ideally, to provide a direct measure of the volume extinction coefficient profile (such as from an HSRL or a Raman lidar) that can be either compared with or incorporated into the MPL retrieval. DOE's guest instrumentation program can provide the avenue for such additional deployments.

Additional desired VAPs include those useful for modeling support. A priority is creating a model forcing data set (or data sets) optimized for cloud and aerosol modeling, such as for the WRF-Chem-based Aerosol Modeling Testbed, and to support adaptation of the LES testbed currently applicable to ARM's Southern Great Plains (SGP) site. The forcing terms needed by LES/CRM models (e.g., horizontal advective tendencies of temperature and moisture, surface fluxes, vertical motion, etc.) are typically included in the ARM variational analysis product (Zhang and Lin, 1997; Zhang et al. 2001). Further modeling-support VAPs such as VARANAL, MergeSonde, and RIPBE will be discussed further. Other VAPs that allow users access to basic quantities such as the cloud boundaries (ARSCL), MFRSR AODs, the shortwave flux analysis, and the new cloud Droplet Number Concentration VAP are also priorities. In further discussions with AeroCom modelers, CLARIFY and ORACLES scientists will attempt to identify integrative data sets across all three campaigns, and particularly data sets that are useful to the AeroCom community. One such example will be to develop (or contribute to development of) an idealized absorbing aerosol distribution as a function of location that can be merged with the Easy Aerosol model intercomparison protocol (Voigt et al. 2013) established for the World Climate Research Program's "Coupling Clouds to Circulation" initiative.

An additional consideration is further analysis of the actual aerosol particles. The chemical composition and morphology of an aerosol particle are critical aspects that control its radiative properties and its ability to activate to form cloud droplets. Whereas some instruments can measure chemical composition and other instruments allow inference of chemical composition or other properties, laboratory analyses such as electron microscopy techniques can provide a wealth of information on chemical composition and morphology that cannot be obtained in other ways.

These require the collection of aerosol samples on filters and storage for later analysis. Although such techniques are time consuming, they provide the necessary detail of information that can be used for source attribution and to infer information on life cycle and processing in the atmosphere. Aerosol particle sampling is typical on many ground sites such as the Interagency Monitoring of Protected Visual Environment stations and the World Meteorological Organization Global Atmospheric Watch sites, and worked well on the Marine ARM GPCI Investigation of Clouds field campaign. Currently, the potential for resources (i.e., technician time, filter samples, etc.) and the desired analyses and protocols for LASIC still need to be determined.

DOE's guest instrumentation program can be used to support additional measurements considered as high priority to the LASIC strategy. Anticipated and desired instrumentation is listed in Table 3. A second lidar is the highest priority of the additional requested instrumentation.

Table 3. Guest instrumentation, anticipated (black) and desired (blue).

Guest Instrumentation	Function
filter sampling	smoke composition
aerosol lidar (HSRL, Raman)	aerosol extinction and moisture profile
Unmanned Aerial Vehicles (UAVs)	spatial characterization of moisture and temperature fields over ocean

Site planning activities will include analysis of available surface-based data sets such as the AERONET data on aerosol properties and surface meteorological data (rain, cloud cover, wind speed, lifting condensation level). A satellite analysis that includes daily/synoptic fluctuations will be done. Analysis of data from the German R/V Polarstern cruise in April 2014 will constitute a first look at the cloud microphysical vertical structure of the southeast Atlantic. For this cruise, researchers from the NOAA-Earth System Research Laboratory, in collaboration with Andreas Macke at the Institute for Tropospheric Research in Leipzig, Germany, deployed a motion-stabilized Doppler W-band cloud radar (Moran et al. 2011) along with a ceilometer and microwave profiler. These instruments complement the Leipzig OCEANET instrumentation suite, which consists of a Raman lidar, microwave radiometer, radiation and turbulent flux measurements, a sun photometer, and rain gauges. Radiosondes were also launched.

5.0 Modeling Plan

Modeling activities are divided by their focus on either the aerosol or the cloud response to the aerosol. Aerosol-focused modeling activities center on improving the currently uncertain treatment of carbonaceous aerosol aging in global models. In the CAM5 model, carbonaceous aerosols are represented either by a single accumulation mode in the simplified three-mode aerosol module (MAM3) or by a primary-carbon mode plus the accumulation mode in a more complex seven-mode aerosol module, called MAM7 (Liu et al. 2011). Black carbon and particulate organic matter (POM) are emitted into the accumulation mode in MAM3 and assumed to immediately mix with any co-existing hygroscopic species, which represents a fast aging process. In the MAM7, BC and POM are emitted into the primary-carbon mode, in which particles have low hygroscopicity and are less susceptible to wet scavenging, and then gradually are transferred to the accumulation mode as they age by condensation of soluble materials and/or coagulation with soluble particles. Therefore, assumptions have to be made for representing the BC and POM aging process in CAM5 (and in other climate models as well). LASIC observations will be applied to evaluate the aging assumptions and to improve the treatment of aging of BB aerosols in CAM5 and other global aerosol-climate models. Along with the recently developed capability of radiation diagnostic calculations (Ghan et al. 2012) and the carbonaceous aerosol source tagging technique in CAM5 (Wang et al. 2014), we will be able to quantify the direct radiative forcing due to BC and POM, respectively, emitted from different BB or fossil fuel combustion sources and to estimate emission uncertainties. The proposed long-term temporally frequent LASIC observations will also allow the study of diurnal and seasonal cycles of BB aerosols and marine low clouds over the southeast Atlantic using the WRF process model and the CAM5 model constrained by reanalysis meteorological products (Ma et al. 2013). Similar to many other climate models, the default CAM5 has systematic biases in predicting the vertical distribution of aerosols and their transport to remote regions. Some recent CAM5 model adjustments in convective transport and wet removal of aerosols by Wang et al. (2013) significantly

improve the horizontal and vertical distribution of BC over many regions, but have not been evaluated for trade-wind cumulus regimes. LASIC data sets will also be incorporated into the larger AeroCom effort, which is now beginning a model intercomparison with a focus on BB aerosols (P. Stier and M. Schultz, personal communications).

Other process-modeling activities address the importance of adequately representing low clouds in climate models (Bony and Dufresne 2005) if we are to understand the one potentially negative feedback to climate change. The southeastern Atlantic is such a region in which cloud feedback on climate change is still highly uncertain (Figure 10). Ascension Island is relatively isolated from mid-latitude synoptic disturbances by its subtropical/tropical location, which helps explain the high annual-mean net cloud radiative forcing relative to the northern hemisphere stratocumulus decks. For this reason, Ascension Island provides a more robust laboratory with which to explore cloud adjustment responses to weak radiative forcings than similar northern hemisphere locations; this has not yet been exploited. Low clouds are almost as poorly represented within climate models with fixed sea surface temperatures as within coupled climate models with high SST biases (Figure 10), indicating that the issue is more in the representation of the internal cloud processes than with the boundary conditions.

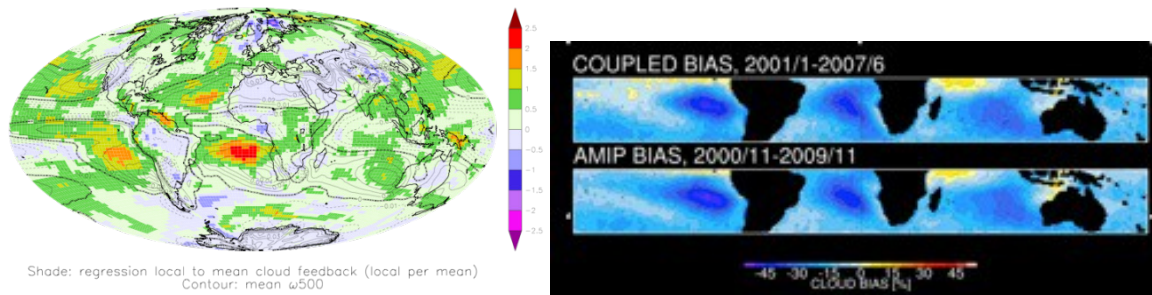


Figure 11. Left-hand panel: CMIP3 Intermodel regression of the local cloud feedback upon the global mean cloud feedback. High values highlight those areas that contribute the most to the intermodel spread in global mean cloud feedback. Contours show the 20-year global mean 500 hPa pressure velocity. Note, this is for $2\times\text{CO}_2$ simulations only, and aerosols are not considered. Modified from Figure 4 of Soden and Vechi (2011), courtesy of Gabriel Vechi. Right-hand panel: Total cloud amount bias in CESM1/CAM5 with respect to the multiangle imaging spectroradiometer satellite-derived cloud fractions when coupled to the ocean (top panel) and atmosphere only (bottom panel). Plot courtesy of Brian Medeiros.

A range of modeling approaches occurring at different scales will be applied to investigate the coupling between aerosols and the low clouds. These span large-eddy simulations that examine detailed cloud and cloud-aerosol processes within relatively small domains and nested within larger-scale domains capable of transmitting a large-scale forcing inward, to the large-scale climate models. The WRF model (Skamarock et al. 2008) will serve as one modeling tool. Its realism as a LES tool or cloud-resolving modeling tool for simulating marine shallow clouds, aerosols, and/or aerosol-cloud interactions has been demonstrated in previous studies (Wang et al. 2009; Wang and Feingold 2009a, b; Lee et al. 2013; Kazil et al. 2011; Yang et al. 2011, 2012; Li et al. 2014). The WRF model (with or without coupled chemistry) will be applied to gain more process-level understanding of the interactions between BB aerosols and shallow clouds under various meteorological conditions near St Helena and Ascension Islands. Aerosol effects on clouds will also be quantified using Lagrangian particle tracing within WRF-Chem (e.g., Brioude et al. 2009).

The WRF model will also serve as a parameterization testbed for which LASIC observations will establish benchmarks. For example, the WRF model can be set up for particular meteorologically distinct days, after which physical parameterizations can be swapped in and out of the model (e.g., Fast et al. 2011). A similar parameterization swap exercise can be applied to single-column models (SCM) derived from climate models, providing a direct link for climate model improvement. SCM modeling will explore the physics within climate models (both with and without aerosol), perturbations to those physics, and the testing of different physical parameterizations (e.g., Neggers et al. 2012). SCM modeling of select case studies will be compared to further assess climate model parameterizations and their sensitivity to the sub-gridscale (e.g., Moeng et al. 1996; Duynkerke et al. 2004; Stevens et al., 2005; Zhu et al. 2005; Wyant et al. 2007).

At the largest scale, parameterization testbed (i.e., DOE Cloud-Associated Parameterizations Testbed), forecasting exercises, which examine the short-range forecasts of global climate models (specifically, CAM5 and new DOE-sponsored Accelerated Climate Model for Energy, which contains most of the CAM5 physics), will assess their fast physics by comparing against the LASIC diurnal cycle measurements. Such analysis will help distinguish robust internal processes from regional differences (e.g., Hannay et al. 2009; Medeiros et al. 2012). Additional comparisons of cloud adjustment effects to aerosol overhead in the forecast framework will gain insight into the sensitivity of the clouds within NCAR's coupled climate model to aerosol effects, and can help establish the framework for broader model participation.

The experience and insights gained with the CAP-MBL data sets will guide similar analyses for the “similar-but-different” trade-wind cumulus intermixed with carbonaceous aerosol regime. The clouds and aerosols sampled at Graciosa have been compared with short-range forecasts made by a variety of models (Wood et al. 2015). A pilot analysis with two climate and two weather forecast models shows that they reproduce the observed time-varying vertical structure of lower-tropospheric clouds fairly well, but the cloud-nucleating aerosol concentrations less well. A similar exercise can be used to assess cloud behavior under varying aerosol loads overhead. The modeling plan needs to be developed in more detail, with collaborative projects identified containing timelines and protocols. Further data integration and utility with the DOE modeling testbeds will be emphasized, and outreach efforts will be made to modeling centers and groups.

6.0 Relevance to U.S. Department of Energy

The mission of the ARM Climate Research Facility is to resolve uncertainties in how clouds and aerosols impact the spatial distribution of the Earth's radiative balance, precipitation, and temperature in global and regional climate simulations and projections. A wide range in top-of-atmosphere aerosol forcing is clearly evident in global aerosol models when absorbing aerosols overlie clouds (Figure 2). The southeastern Atlantic Ocean therefore represents a stringent testing ground for models: the magnitude and geographic distribution of the aerosol optical depth, wavelength-dependent aerosol SSA, aerosol vertical profile, geographic distribution of the cloud, cloud fraction, cloud liquid water content, cloud droplet effective radii, and cloud vertical profile must all be accurately reproduced. Similarly, uncertainties associated with both the aerosol semi-direct and indirect effects are significant, particularly as the degree of mixing of aerosol and cloud is highly uncertain.

The stratus and trade-wind cumulus regimes are being characterized through campaign measurements from DOE ARM Climate Research Facilities such as the Clouds, Aerosols, Precipitation in the Marine Boundary Layer (CAP-MBL; Wood et al. 2015) at the Azores Islands (37° N, 25° W) in the suppressed northern Atlantic Ocean. This is now the fixed Eastern North Atlantic ARM site dedicated to improving our understanding of boundary-layer processes. The southeastern Pacific stratocumulus regime was sampled during VOCALS. A mobile deployment (MAGIC) is providing unprecedented observations of the California to Hawaii stratus-to-cumulus transition. However, the ARM Facility has not yet gathered observations within an almost exclusively tradewind-cumulus environment, and only a few within the southern hemisphere (restricted to the VOCALS aircraft campaign), but none within a region with a positive top-of-atmosphere forcing due to the presence of absorbing aerosols. Long-term measurements at high time resolution are completely lacking from the region, with available measurements limited to basic measurements made during SAFARI-2000. Since 2000, models with a range of resolutions have developed, and new surface-based technologies have opened up new research horizons. The recent development of scanning cloud radars and the very new solar array spectrometers provide new opportunities for examining heretofore-unexamined science questions for the ARM Facility. The remote, strategic location of Ascension Island is particularly valuable for inferring the impacts of aged carbonaceous aerosol representative of a large area and for furthering ARM's goals of improving our understanding and representation of low-cloud behavior within the climate system.

7.0 References

- Abel, SJ, JM Haywood, EJ Highwood, J Li, and PR Buseck. 2003. “Evolution of biomass burning aerosol properties from an agricultural fire in southern Africa.” *Geophysical Research Letters* 30(15): 1783, [doi:10.1029/2003GL017342](https://doi.org/10.1029/2003GL017342).
- Abel, SJ, EJ Highwood, J Haywood, and M Stringer. 2005. “The direct radiative effect of biomass burning aerosol over southern Africa.” *Atmospheric Chemistry and Physics* 5: 1999-2018, [doi:10.5194/acp-5-1999-2005](https://doi.org/10.5194/acp-5-1999-2005).
- Ackerman, AS, OB Toon, DE Stevens, AJ Heymsfield, V Ramanathan, and EJ Welton. 2000. “Reduction of tropical cloudiness by soot.” *Science* 288: 1042-1047, [doi:10.1126/science.288.5468.1042](https://doi.org/10.1126/science.288.5468.1042).
- Adebisi, A, P Zuidema, and SJ Abel. 2015. “The convolution of dynamics and moisture with the presence of shortwave absorbing aerosols over the southeast Atlantic.” *Journal of Climate*, 28: 1997-2024, [doi:10.1175/JCLI-D-14-00352.1](https://doi.org/10.1175/JCLI-D-14-00352.1).
- Adebisi, A and P Zuidema, 2016. “The role of the southern African easterly jet in modifying the southeast Atlantic aerosol and cloud environments.” *Quarterly Journal of the Royal Meteorological Society*, revised pending acceptance
- Akagi, SK, JS Craven, JW Taylor, GR McMeeking, RJ Yokelson, IR Burling, SP Urbanski, CE Wold, JH Seinfeld, H Coe, MJ Alvarado, and DR Weise. 2012. “Evolution of trace gases and particles emitted by a chaparral fire in California.” *Atmospheric Chemistry and Physics* 12: 1397-1421, [doi:10.5194/acp-12-1397-2012](https://doi.org/10.5194/acp-12-1397-2012).
- Alvarado, MJ, and RG Prinn, 2008. “Formation of ozone and growth of aerosols in young smoke plumes from biomass burning, part 1: Lagrangian parcel studies.” *Journal of Geophysical Research* 114: D09306, [doi:10.1029/2008JD011144](https://doi.org/10.1029/2008JD011144).
- Alvarado, MJ, CR Lonsdale, RJ Yokelson, SK Akagi, H Coe, JS Craven, EV Fischer, GR McMeeking, JH Seinfeld, T Soni, JW Taylor, DR Weise, and CE Wold. 2015. “Investigating the links between ozone and organic aerosol chemistry in a biomass burning plume from a prescribed fire in California chaparral.” *Atmospheric Chemistry and Physics* 15: 6667-6688, [doi:10.5194/acp-15-6667-2015](https://doi.org/10.5194/acp-15-6667-2015).
- Andreae, MO and D Rosenfeld. 2008. “Aerosol-cloud-precipitation interactions. Part 1: The nature and sources of cloud-active aerosols.” *Earth-Science Reviews* 89: 13-41, [doi:10.1016/j.earscirev.2008.03.001](https://doi.org/10.1016/j.earscirev.2008.03.001).
- Bellouin, N, GW Mann, MT Woodhouse, C Johnson, KS Carslaw, and M Dalvi. 2013. “Impact of the modal aerosol scheme GLOMAP-mode on aerosol forcing in the Hadley Centre Global Environmental Model.” *Atmospheric Chemistry and Physics* 13: 3027-3044, [doi:10.5194/acp-13-3027-2013](https://doi.org/10.5194/acp-13-3027-2013).
- Bennartz, R. 2007. “Global assessment of marine boundary layer cloud droplet number concentration from satellite.” *Journal of Geophysical Research* 112: D02201, [doi:10.1029/2006JD007547](https://doi.org/10.1029/2006JD007547).
- Bond, TC, SJ Doherty, DW Fahey, PM Forster, T Berntsen, BJ DeAngelo, MG Flanner, S Ghan, B Kärcher, D Koch, S Kinne, Y Kondo, PK Quinn, MC Sarofim, MG Schultz, M Schulz, C Venkataraman,

- H Zhang, S Zhang, N Bellouin, SK Guttikunda, PK Hopke, MZ Jacobson, JW Kaiser, Z Klimont, U Lohmann, JP Schwarz, D Shindell, T Storelvmo, SG Warren, and CS Zender. 2013. “Bounding the role of black carbon in the climate system: A scientific assessment.” *Journal of Geophysical Research* 118:5 380-5552, [doi:10.1002/jgrd.50171](https://doi.org/10.1002/jgrd.50171).
- Borque, P, P Kollias, and S Giangrande. 2014. “First observations of tracking clouds using scanning ARM cloud radars.” *Journal of Applied Meteorology and Climatology* 53: 2732-2746, [doi:10.1175/JAMC-D-130182.1](https://doi.org/10.1175/JAMC-D-130182.1).
- Boucher, O, D Randall, P Artaxo, C Bretherton, G Feingold, P Forster, V-M Kerminen, Y Kondo, H Liao, U Lohmann, P Rasch, SK Satheesh, S Sherwood, B Stevens, and X-Y Zhang. 2013. “Clouds and aerosols.” In *Climate Change 2013: The Physical Science Basis. Contribution of Working Group I to the Fifth Assessment Report of the Intergovernmental Panel on Climate Change*, TF Stocker, D Qin, G-K Plattner, M Tignor, SK Allen, J Boschung, A Nauels, Y Xia, V Bex, and PM Midgley (editors), Cambridge University Press, Cambridge, United Kingdom and New York, NY, USA, pp.571-657.
- Brioude, J, OR Cooper, G Feingold, M Trainer, SR Freitas, D Kowal, JK Ayers, E Prins, P Minnis, SA McKeen, GJ Frost, and EY Hsie. 2009. “Effect of biomass burning on marine stratocumulus clouds off of the Californian coast.” *Atmospheric Chemistry and Physics* 9: 8841-8856, [doi:10.5194/acp-10-8841-2009](https://doi.org/10.5194/acp-10-8841-2009).
- Brioude, J, WM Angevine, R Ahmadov, S-W Kim, S Evan, SA McKeen, E-Y Hsie, GJ Frost, JA Neuman, IB Pollack, J Peischl, TB Ryerson, J Holloway, SS Brown, JB Nowak, JM Roberts, SC Wofsy, GW Santoni, T Oda, and M Trainer. 2013. “Top-down estimate of surface flux in the Los Angeles Basin using a mesoscale inverse modeling technique: assessing anthropogenic emissions of CO, NO_x and CO₂ and their impacts.” *Atmospheric Chemistry and Physics* 13: 3661-3677, [doi:10.5194/acp-13-3661-2013](https://doi.org/10.5194/acp-13-3661-2013).
- Chand, D, R Wood, TL Anderson, SK Satheesh, and RJ Charlson. 2009. “Satellite-derived direct radiative effect of aerosols dependent on cloud cover.” *Nature Geoscience* 2: 181-184, [doi:10.1038/ngeo0437](https://doi.org/10.1038/ngeo0437).
- Chiu, JC, A Marshak, C-H Huang, T Varnai, RJ Hogan, DM Giles, BN Holben, EJ O'Connor, Y Knyazikhin, and WJ Wiscombe. 2012. “Cloud droplet size and liquid water path retrievals from zenith radiance measurements: Examples from the Atmospheric Radiation Measurement Program and the Aerosol Robotic Network.” *Atmospheric Chemistry and Physics* 12, [doi:10.5194/acp-12-10313-2012](https://doi.org/10.5194/acp-12-10313-2012).
- Costantino, L and FM Bréon. 2010. “Analysis of aerosol-cloud interaction from multi-sensor satellite observations.” *Geophysical Research Letters* 37: L11801, [doi:10.1029/2009GL041828](https://doi.org/10.1029/2009GL041828).
- Costantino L and FM Bréon. 2013. “Aerosol indirect effect on warm clouds over South-East Atlantic, from co-located MODIS and CALIPSO observations.” *Atmospheric Chemistry and Physics* 13: 69–88, [doi:10.5194/acp-13-69-2013](https://doi.org/10.5194/acp-13-69-2013).
- de Graaf, M, LG Tilstra, P Wang, and P Stammes. 2012. “Retrieval of the aerosol direct radiative effect over clouds from spaceborne spectrometry.” *Journal of Geophysical Research* 117: D07207, [doi:10.1029/2011JD017160](https://doi.org/10.1029/2011JD017160).

- de Graaf, M, N Bellouin, LG Tilstra, J Haywood, and P Stammes. 2014. "Aerosol direct radiative effect of smoke over clouds over the southeast Atlantic Ocean from 2006 to 2009." *Geophysical Research Letters* 41: 7723-7730, [doi:10.1002/2014GL061103](https://doi.org/10.1002/2014GL061103).
- Duynkerke, PG, SR de Roode, MC van Zanten, J Calvo, J Cuxart, S Cheinet, A Chlond, H Grenier, PJ Jonker, M Köhler, G Lenderink, D Lewellen, C-L Lappen, AP Lock, C-H Moeng, F Mueller, D Olmeda, J-M Piriou, E Sanchez, and I Sednev. 2004. "Observations and numerical simulations of the diurnal cycle of the EUROCS stratocumulus case." *Quarterly Journal of the Royal Meteorological Society* 130: 3269-3296, [doi:10.1256/qj.03.139](https://doi.org/10.1256/qj.03.139).
- Eck, TF, BN Holben, JS Reid, MM Mukelabai, SJ Piketh, O Torres, HT Jethva, EJ Hyer, DE Ward, O Dubovik, A Sinyuk, JS Schafer, DM Giles, M Sorokin, A Smirnov, and I Slutsker. 2013. "A seasonal trend of single scattering albedo in southern African biomass-burning particles: implications for satellite products and estimates of emissions for the world's largest biomass-burning source." *Journal of Geophysical Research: Atmospheres* 118: 6414-6432, [doi:10.1002/jgrd.50500](https://doi.org/10.1002/jgrd.50500).
- Fang, M, RJ Doviak, and BA Albrecht. 2012. "Analytical expressions for Doppler spectra of scatter from hydrometeors observed with a vertically directed radar beam." *Journal of Atmospheric and Oceanic Technology* 29: 500-509, [doi:10.1175/JTECH-D-11-00005.1](https://doi.org/10.1175/JTECH-D-11-00005.1).
- Fast, JD, WI Gustafson Jr., EG Chapman, RC Easter, JP Rishel, RA Zaveri, GA Grell, and MC Barth. 2011. "The aerosol modeling testbed: A community tool to objectively evaluate aerosol process modules." *Bulletin of the American Meteorological Society* 92: 343-360, [doi:10.1175/2010BAMS2868.1](https://doi.org/10.1175/2010BAMS2868.1).
- Feingold, G, H Jiang, and JY Harrington. 2005. "On smoke suppression of clouds in Amazonia." *Geophysical Research Letters* 32(2): L02804, [doi:10.1029/2004GL021369](https://doi.org/10.1029/2004GL021369).
- Feingold, G and H Siebert. 2009. "Cloud-aerosol interactions from the micro to the cloud scale." In Strungmann Forum Report, *Clouds in the Perturbed Climate System: Their Relationship to Energy Balance, Atmospheric Dynamics, and Precipitation*, J Heintzenberg and RJ Charlson (editors), Chapter 14, vol. 2, The MIT Press, Cambridge, Massachusetts, [doi:10.7551/mitpress/9780262012874.001.0001](https://doi.org/10.7551/mitpress/9780262012874.001.0001).
- Garstang, M, PD Tyson, R Swap, M Edwards, P Kållberg, and JA Lindesay. 1996. "Horizontal and vertical transport of air over southern Africa." *Journal of Geophysical Research* 101(D19): 23721-23736, [doi:10.1029/95JD00844](https://doi.org/10.1029/95JD00844).
- Ghan, SJ, X Liu, RC Easter, R Zaveri, PJ Rasch, J-H Yoon, and B Eaton. 2012. "Toward a minimal representation of aerosols in climate models: comparative decomposition of aerosol direct, semidirect, and indirect radiative forcing." *Journal of Climate* 25: 6461-6476, [doi:10.1175/JCLI-D-11-00650.1](https://doi.org/10.1175/JCLI-D-11-00650.1).
- Granier, C, B Bessagnet, T Bond, A D'Angiola, HD van der Gon, GJ Frost, A Heil, JW Kaiser, S Kinne, Z Klimont, S Kloster, J-F Lamarque, C Liousse, T Masui, F Meleux, A Mieville, T Ohara, J-C Raut, K Riahi, MG Schultz, SJ Smith, A Thompson, J van Aardenne, GR van der Werf, and DP van Vuuren. 2011. "Evolution of anthropogenic and biomass burning emissions of air pollutants at global and regional scales during the 1980–2010 period." *Climatic Change* 109: 163-190, [doi:10.1007/s10584-011-0154-1](https://doi.org/10.1007/s10584-011-0154-1).

- Hannay, C, DL Williamson, JJ Hack, JT Kiehl, JG Olson, SA Klein, CS Bretherton, and M Koehler. 2009. "Evaluation of forecasted southeast Pacific stratocumulus in the NCAR, GFDL, and ECMWF models." *Journal of Climate* 22: 2871-2889, [doi:10.1175/2008JCLI2479.1](https://doi.org/10.1175/2008JCLI2479.1).
- Haywood, JM and KP Shine. 1995. "The effect of anthropogenic sulfate and soot on the clear sky planetary radiation budget." *Geophysics Research Letters* 22: 603-606, [doi:10.1029/95GL00075](https://doi.org/10.1029/95GL00075).
- Haywood, JM, SR Osborne, PN Francis, A Keil, P Formenti, MO Andreae, and PH Kaye. 2003. "The mean physical and optical properties of regional haze dominated by biomass burning aerosol measured from the C-130 aircraft during SAFARI 2000." *Journal of Geophysical Research* 108: 8473, [doi:10.1029/2002JD002226](https://doi.org/10.1029/2002JD002226).
- Haywood, JM, SR Osborne, and SJ Abel. 2004. "The effect of overlying absorbing aerosol layers on remote sensing retrievals of cloud effective radius and cloud optical depth." *Quarterly Journal of the Royal Meteorological Society* 130: 779-800, [doi:10.1256/qj.03.100](https://doi.org/10.1256/qj.03.100).
- Hill, AA and S Dobbie. 2008. The impact of aerosols on non-precipitating marine stratocumulus. II: the semi-direct effect." *Quarterly Journal of the Royal Meteorological Society* 134: 1155-1165, [doi:10.1002/qj.277](https://doi.org/10.1002/qj.277).
- Hobbs, PV, P Sinha, RJ Yokelson, TJ Christian, DR Blake, S Gao, TW Kirchstetter, T Novakov, and P Pilewskie. 2003. "Evolution of gases and particles from a savanna fire in South Africa." *Journal of Geophysical Research* 108(D13): 8485, [doi:10.1029/2002JD002352](https://doi.org/10.1029/2002JD002352).
- Holben, BN, D Tanré, A Smirnov, TF Eck, I Slutsker, N Abuhassan, WW Newcomb, JS Schafer, B Chatenet, F Lavenu, YJ Kaufman, J Vande Castle, A Setzer, B Markham, D Clark, R Frouin, R Halthore, A Karneli, NT O'Neill, C Pietras, RT Pinker, K Voss, and G Zibordi. 2001. "An emerging ground-based aerosol climatology: aerosol optical depth from AERONET." *Journal of Geophysical Research* 106(D11): 12067-12097, [doi:10.1029/2001JD900014](https://doi.org/10.1029/2001JD900014).
- Intergovernmental Panel on Climate Change (IPCC). 2014. *Climate Change 2013: The Physical Science Basis. Contribution of Working Group I to the Fifth Assessment Report of the Intergovernmental Panel on Climate Change*. TF Stocker, D Qin, G-K Plattner, M Tignor, SK Allen, J Boschung, A Nauels, Y Xia, V Bex, and PM Midgley (eds.), Cambridge University Press, Cambridge, United Kingdom and New York. http://www.ipcc.ch/report/ar5/wg1/docs/WG1AR5_FactSheet.pdf
- Johnson, BT, KP Shine, and PM Forster. 2004. "The semi-direct aerosol effect: Impact of absorbing aerosols on marine stratocumulus." *Quarterly Journal of the Royal Meteorological Society* 130: 1407-1422, [doi:10.1256/qj.03.61](https://doi.org/10.1256/qj.03.61).
- Johnson, BT. 2005. "Large-eddy simulations of the semidirect aerosol effect in shallow cumulus regimes." *Journal of Geophysical Research* 110: D14206, [doi:10.1029/2004JD005601](https://doi.org/10.1029/2004JD005601).
- Kassianov, EI, CJ Flynn, TP Ackerman, and JC Barnard. 2007. "Aerosol single-scattering albedo and asymmetry parameter from MFRSR observations during the ARM Aerosol IOP 2003." *Atmospheric Chemistry and Physics* 7: 3341-3351, [doi:10.5194/acp-7-3341-2007](https://doi.org/10.5194/acp-7-3341-2007).

- Kazil, J, H Wang, G Feingold, AD Clarke, JR Snider, and AR Bandy. 2011. "Modeling chemical and aerosol processes in the transition from closed to open cells during VOCALS-Rex." *Atmospheric Chemistry and Physics* 11: 7491-7514, [doi:10.5194/acp-11-7491-2011](https://doi.org/10.5194/acp-11-7491-2011).
- Kindel, BC, P Pilewskie, KS Schmidt, O Coddington, and MD King. 2011. "Solar spectral absorption by marine stratus clouds: Measurements and modeling." *Journal of Geophysical Research* 116: D10203, [doi:10.1029/2010JD015071](https://doi.org/10.1029/2010JD015071).
- Kinne, S, D O'Donnel, P Stier, S Kloster, K Zhang, H Schmidt, S Rast, M Giorgetta, TF Eck, and B Stevens. 2013. "MAC-v1: A new global aerosol climatology for climate studies." *Journal of Advances in Modeling Earth Systems* 5(4): 704-740, [doi:10.1002/jame.20035](https://doi.org/10.1002/jame.20035).
- Klein, SA and DL Hartmann. 1993. "The seasonal cycle of low stratiform clouds." *Journal of Climate* 6: 1587-1606, [doi:10.1175/1520-0442\(1993\)006<1587:TSCOLS>2.0.CO;2](https://doi.org/10.1175/1520-0442(1993)006<1587:TSCOLS>2.0.CO;2).
- Klein, S. 1997. "Synoptic variability of low-cloud properties and meteorological parameters in the subtropical trade wind boundary layer." *Journal of Climate* 10: 2018-2039, [doi:10.1175/1520-0442\(1997\)010<2018:SVOLCP>2.0.CO;2](https://doi.org/10.1175/1520-0442(1997)010<2018:SVOLCP>2.0.CO;2).
- Koch, D and AD Del Genio. 2010. "Black carbon semi-direct effects on cloud cover: Review and synthesis." *Atmospheric Chemistry and Physics* 10: 7685-7696, [doi:10.5194/acp-10-7685-2010](https://doi.org/10.5194/acp-10-7685-2010).
- Koffi, B, M Schulz, F-M Bréon, J Griesfeller, D Winker, Y Balkanski, S Bauer, T Berntsen, M Chin, WD Collins, F Dentener, T Diehl, R Easter, S Ghan, P Ginoux, S Gong, LW Horowitz, T Iversen, A Kirkevåg, D Koch, M Krol, G Myhre, P Stier, and T Takemura. 2012. "Application of the CALIOP layer product to evaluate the vertical distribution of aerosols estimated by global models: AeroCom phase I results." *Journal of Geophysical Research* 117: D10201, [doi:10.1029/2011JD016858](https://doi.org/10.1029/2011JD016858).
- Kollias, P, J Remillard, E Luke, and W Szyrmer. 2011a. "Cloud radar Doppler spectra in drizzling stratiform clouds: 1. Forward modeling and remote sensing applications." *Journal of Geophysical Research-Atmospheres* 116(D13), [doi:10.1029/2010JD015237](https://doi.org/10.1029/2010JD015237).
- Kollias P, W Szyrmer, J Remillard, and E Luke. 2011b. "Cloud radar Doppler spectra in drizzling stratiform clouds: 2. Observations and microphysical modeling of drizzle evolution." *Journal of Geophysical Research-Atmospheres*, 116(D13), [doi:10.1029/2010JD015238](https://doi.org/10.1029/2010JD015238).
- Kollias, P, N Bharadwaj, K Widener, I Jo, and K Johnson. 2014a. "Scanning ARM cloud radars. Part I: Operational sampling strategies." *Journal of Atmospheric and Oceanic Technologies* 31: 569-582, [doi:10.1175/JTECH-D-13-00044.1](https://doi.org/10.1175/JTECH-D-13-00044.1).
- Kollias, P, I Jo, P Borque, A Tatarevic, K Lamer, N Bharadwaj, K Widener, K Johnson, and EE Clothiaux. 2014b. "Scanning ARM cloud radars. Part II: Data quality control and processing." *Journal of Atmospheric and Oceanic Technologies* 31: 583-598, [doi:10.1175/JTECH-D-13-00045.1](https://doi.org/10.1175/JTECH-D-13-00045.1).
- Koren, I, YJ Kaufman, LA Remer, and JV Martins. 2004. "Measurement of the effect of Amazon smoke on inhibition of cloud formation." *Science* 303: 1342-1345, [doi:10.1126/science.1089424](https://doi.org/10.1126/science.1089424).

- Lamer, K, A Tatarevic, I Jo, and P Kollias. 2013. "Evaluation of gridded Scanning ARM Cloud Radar reflectivity observations and vertical Doppler velocity retrievals." *Atmospheric Measurement Techniques Discussion* 6: 9579-9621, [doi:10.5194/amtd-6-9579-2013](https://doi.org/10.5194/amtd-6-9579-2013).
- Leahy, L. V., T. L. Anderson, T. F. Eck, and R. W. Bergstrom. 2007. "A synthesis of single scattering albedo of biomass burning aerosol over southern Africa during SAFARI 2000." *Geophysical Research Letters* 34, doi:10.1029/2007GL029697.
- Lee, S-S, G Feingold, and PY Chuang. 2012. "Effect of aerosol on cloud-environment interactions in trade cumulus." *Journal of Atmospheric Science* 69: 3607-3632, [doi:10.1175/JAS-D-12-026.1](https://doi.org/10.1175/JAS-D-12-026.1).
- Li, Z, P Zuidema, and P Zhu. 2014. "Simulated convective invigoration processes at trade-wind cumulus cold pool boundaries." *Journal of Atmospheric Science* 71: 2823-2841, [doi:10.1175/JAS-D-13-0184.1](https://doi.org/10.1175/JAS-D-13-0184.1).
- Lin, B, P Minnis, T-F Fan, Y Hu, and W Sun. 2010. "Radiation characteristics of low and high clouds in different oceanic regions observed by CERES and MODIS." *International Journal of Remote Sensing* 31(24): 6473-6492, [doi:10.1080/01431160903548005](https://doi.org/10.1080/01431160903548005).
- Liu, X, RC Easter, SJ Ghan, R Zaveri, P Rasch, X Shi, J-F Lamarque, A Gettelman, H Morrison, F Vitt, A Conley, S Park, R Neale, C Hannay, AML Ekman, P Hess, N Mahowald, W Collins, MJ Iacono, CS Bretherton, MG Flanner, and D Mitchell. 2011. "Toward a minimal representation of aerosol direct and indirect effects: model description and evaluation." *Geoscientific Model Development Discussions* 4(4): 485-3598, [doi:10.5194/gmdd-4-3485-2011](https://doi.org/10.5194/gmdd-4-3485-2011).
- Loeb, NG and GL Schuster. 2008. "An observational study of the relationship between cloud, aerosol and meteorology in broken low-level cloud conditions." *Journal of Geophysical Research* 113: D14214, [doi:10.1029/2007JD009763](https://doi.org/10.1029/2007JD009763).
- Ma, P-L, PJ Rasch, H Wang, K Zhang, RC Easter, S Tilmes, JD Fast, X Liu, J-H Yoon, and J-F Lamarque. 2013. "The role of circulation features on black carbon transport into the Arctic in the Community Atmosphere Model version 5 (CAM5)." *Journal of Geophysical Research* 118(10): 4657-4669, [doi:10.1002/jgrd.50411](https://doi.org/10.1002/jgrd.50411).
- Magi, B. I., Q. Fu, J. Redemann, and B. Schmid. 2008. "Using aircraft measurements to estimate the magnitude and uncertainty of the shortwave direct radiative forcing of southern African biomass burning aerosol." *Journal of Geophysical Research* 113: D05213, doi:10.1029/2007JD009258
- McFarquhar, GM, S Platnick, L Di Girolamo, H Wang, G Wind, and G Zhao. 2004. "Trade wind cumuli statistics in clean and polluted air over the Indian Ocean from in situ and remote sensing measurements." *Geophysical Research Letters* 31: L21105, [doi:10.1029/2004GL020412](https://doi.org/10.1029/2004GL020412).
- McFarquhar, GM and H Wang. 2006. "Effects of aerosols on trade wind cumuli over the Indian Ocean: model simulations." *Quarterly Journal of the Royal Meteorological Society* 132: 821-843, [doi:10.1256/qj.04.179](https://doi.org/10.1256/qj.04.179).
- Mann, GW, KS Carslaw, DV Spracklen, DA Ridley, PT Manktelow, MP Chipperfield, SJ Pickering, and CE Johnson. 2010. "Description and evaluation of GLOMAP-mode: a modal global aerosol microphysics

model for the UKCA composition-climate model.” *Geoscientific Model Development* 3: 519-551, [doi:10.5194/gmd-3-519-2010](https://doi.org/10.5194/gmd-3-519-2010).

Mann, JAL, JC Chiu, RJ Hogan, EJ O'Connor, TS L'Ecuyer, THM Stein, and A Jefferson. 2014. “Aerosol impacts on drizzle properties in warm clouds from ARM Mobile Facility maritime and continental deployments.” *Journal of Geophysical Research–Atmospheres* 119: 4136-4148, [doi:10.1002/2013JD021339](https://doi.org/10.1002/2013JD021339).

Mauger, GS and JR Norris. 2007. “Meteorological bias in satellite estimates of aerosol-cloud relationships.” *Geophysical Research Letters* 34: L16824, [doi:10.1029/2007GL029952](https://doi.org/10.1029/2007GL029952).

Mechoso, CR, R Wood, R Weller, CS Bretherton, AD Clarke, H Coe, C Fairall, JT Farrar, G Feingold, R Garreaud, C Grados, J McWilliams, SP de Szoeke, SE Yuter, and P Zuidema. 2014. “Ocean-cloud-atmosphere-land interactions in the Southeast Pacific: the VOCALS program.” *Bulletin of the American Meteorological Society* 95: 357-375, [doi:10.1175/BAMS-D-11-00246.1](https://doi.org/10.1175/BAMS-D-11-00246.1).

Medeiros, B, DL Williamson, C Hannay, and JG Olson. 2012. “Southeast Pacific stratocumulus in the Community Atmosphere Model.” *Journal of Climate* 25: 6175-6192, [doi:10.1175/JCLI-D-11-00503.1](https://doi.org/10.1175/JCLI-D-11-00503.1).

Meyer, K, S Platnick, L Oreopoulos, and D Lee. 2013. “Estimating the direct radiative forcing of absorbing aerosols overlying marine boundary layer clouds in the southeast Atlantic using MODIS and CALIOP.” *Journal of Geophysical Research* 118(10): 4801-4815, [doi:10.1002/jgrd.50449](https://doi.org/10.1002/jgrd.50449).

Mlawer, EJ, PD Brown, SA Clough, LC Harrison, JJ Michalsky, PW Kiedron, and T Shippert. 2000. “Comparison of spectral direct and diffuse solar irradiance measurements and calculations for cloud-free conditions.” *Geophysical Research Letters* 27: 2653-2656, [doi:10.1029/2000GL011498](https://doi.org/10.1029/2000GL011498).

Moeng, C-H, WR Cotton, C Bretherton, A Chlond, M Khairoutdinov, S Krueger, WS Lewellen, MK MacVean, JRM Pasquier, HA Rand, AP Siebesma, B Stevens, and RI Sykes. 1996. “Simulation of a stratocumulus-topped planetary boundary layer: intercomparison among different numerical codes.” *Bulletin of the American Meteorological Society* 77: 261-278, [doi:10.1175/1520-0477\(1996\)077<261:SOASTP>2.0.CO;2](https://doi.org/10.1175/1520-0477(1996)077<261:SOASTP>2.0.CO;2).

Moran, KP, S Pezoa, C Fairall, C Williams, T Ayers, A Brewer, SP de Szoeke, and V Ghate. 2011. “A motion-stabilized W-band radar for shipboard observations of marine boundary-layer clouds.” *Boundary Layer Meteorology* 143(1), [doi:10.1007/s10546-011-9674-5](https://doi.org/10.1007/s10546-011-9674-5).

Myrhe, G, BH Samset, M Schulz, Y Balkanski, S Bauer, TK Berntsen, H Bian, N Bellouin, M Chin, T Diehl, RC Easter, J Feichter, SJ Ghan, D Hauglustaine, T Iversen, S Kinne, A Kirkevåg, J-F Lamarque, G Lin, X Liu, MT Lund, G Luo, X Ma, T van Noije, JE Penner, PJ Rasch, A Ruiz, Ø Seland, RB Skeie, P Stier, T Takemura, K Tsigaridis, P Wang, Z Wang, L Xu, H Yu, F Yu, J-H Yoon, K Zhang, H Zhang, and C Zhou. 2013. “Radiative forcing of the direct aerosol effect from AeroCom Phase II simulations.” *Atmospheric Chemistry and Physics* 13: 1853-1877, [doi:10.5194/acp-13/1853-2013](https://doi.org/10.5194/acp-13/1853-2013).

Neggers, RAJ, AP Siebesma, and T Heus. 2012. “Continuous single-column model evaluation at a permanent meteorological supersite.” *Bulletin of the American Meteorological Society* 93: 1389-1400, [doi:10.1175/BAMS-D-11-00162.1](https://doi.org/10.1175/BAMS-D-11-00162.1).

- Noda, AT and M Satoh. 2014. “Intermodel variances of subtropical stratocumulus environments simulated in CMIP5 models.” *Geophysical Research Letters* 41: 7754-7761, [doi:10.1002/2014GL061812](https://doi.org/10.1002/2014GL061812).
- Öktem, R, J Lee, Prabhat, J Lee, A Thomas, P Zuidema, and DM Romps. 2014. “Stereophotogrammetry of oceanic clouds.” *Journal of Atmospheric and Oceanic Technology* 31: 1482-1501, [doi:10.1175/JTECH-D-13-00224.1](https://doi.org/10.1175/JTECH-D-13-00224.1).
- Painemal, D and P Zuidema. 2011. “Assessment of MODIS cloud effective radius and optical thickness retrievals over the Southeast Pacific with VOCALS-REx in situ measurements.” *Journal of Geophysical Research* 116: D24206, [doi:10.1029/2011JD016155](https://doi.org/10.1029/2011JD016155).
- Painemal, D, S Kato, and P Minnis. 2014. “Boundary layer regulation in the southeast Atlantic cloud microphysics during the biomass burning season as seen by the A-train satellite constellation.” *Journal of Geophysical Research* 119: 11288-11302, [doi:10.1002/2014JD022182](https://doi.org/10.1002/2014JD022182).
- Painemal, D, K-M Xu, A Cheng, P Minnis, and R Palikonda. 2015. “Mean structure and diurnal cycle of Southeast Atlantic boundary layer clouds: insights from satellite observations and multiscale modeling framework simulations.” *Journal of Climate* 28(1): 324–341, [doi:10.1175/JCLI-D-14-00368.1](https://doi.org/10.1175/JCLI-D-14-00368.1).
- Petters, JL, H Jiang, G Feingold, DL Rossiter, D Khelif, LC Sloan, and PY Chuang. 2013. “A comparative study of the response of modeled non-drizzling stratocumulus to meteorological and aerosol perturbations.” *Atmospheric Chemistry and Physics* 13: 2507-2529, [doi:10.5194/acp-13-2507-2013](https://doi.org/10.5194/acp-13-2507-2013).
- Ramanathan, V and G Carmichael. 2008. “Global and regional climate changes due to black carbon.” *Nature Geoscience* 1: 221-227, [doi:10.1038/ngeo156](https://doi.org/10.1038/ngeo156).
- Randles, CA and V Ramaswamy. 2010. “Direct and semi-direct impacts of absorbing biomass burning aerosol on the climate of southern Africa: a Geophysical Fluid Dynamics Laboratory GCM sensitivity study.” *Atmospheric Chemistry and Physics* 10:9819-9831, [doi:10.5194/acp-10-9819-2010](https://doi.org/10.5194/acp-10-9819-2010).
- Remer, LA. 2009. “Atmospheric science: Smoke above clouds.” *Nature Geoscience* 2: 167-168, [doi:10.1038/ngeo456](https://doi.org/10.1038/ngeo456).
- Rémillard, J, P Kollias, E Luke, and R Wood. 2012. “Marine boundary layer cloud observations in the Azores.” *Journal of Climate* 25: 7381-7398, [doi:10.1175/JCLI-D-11-00610.1](https://doi.org/10.1175/JCLI-D-11-00610.1).
- Ross, KE, SJ Piketh, RT Bruintjes, RP Burger, RJ Swap, and HJ Annegarn. 2003. “Spatial and seasonal variations in CCN distribution and the aerosol-CCN relationship over Southern Africa.” *Journal of Geophysical Research* 108: 8481, [doi:10.1029/2002JD002384](https://doi.org/10.1029/2002JD002384).
- Russell, PB, SA Kinne, and RW Bergstrom. 1997. “Aerosol climate effects: local radiative forcing and column closure experiments.” *Journal of Geophysical Research* 102: 9397-9407, [doi:10.1029/97JD00112](https://doi.org/10.1029/97JD00112).
- Sakaeda, N, R Wood, and PJ Rasch. 2011. “Direct and semi-direct aerosol effects of southern African biomass-burning aerosol.” *Journal of Geophysical Research* 116: D12205, [doi:10.1029/2010JD015540](https://doi.org/10.1029/2010JD015540).

- Sandu, I, B Stevens, and R Pincus. 2010. “On the transitions in marine boundary layer cloudiness.” *Atmospheric Chemistry and Physics* 10: 2377-2391, [doi:10.5194/acp-10-2377-2010](https://doi.org/10.5194/acp-10-2377-2010).
- Satheesh, SK, O Torres, LA Remer, SS Babu, V Vinoj, TF Eck, RG Kleidman, and BN Holben. 2009. “Improved assessment of aerosol absorption using OMI-MODIS joint retrieval.” *Journal of Geophysical Research* 114: D05209, [doi:10.1029/2008JD011024](https://doi.org/10.1029/2008JD011024).
- Schmidt, KS, G Feingold, P Pilewskie, H Jiang, O Coddington, and M Wendisch. 2009. “Irradiance in polluted cumulus fields: measured and modeled cloud-aerosol effects.” *Geophysical Research Letters* 36: L07804, [doi:10.1029/2008GL036848](https://doi.org/10.1029/2008GL036848).
- Schmidt, KS, P Pilewskie, R Bergstrom, O Coddington, J Redemann, J Livingston, P Russell, E Bierwirth, M Wendisch, W Gore, MK Dubey, and C Mazzoleni. 2010. “A new method for deriving aerosol solar radiative forcing and its first application within MILAGRO/INTEx-B.” *Atmospheric Chemistry and Physics* 10: 7829-7843, [doi:10.5194/acp-10-7829-2010](https://doi.org/10.5194/acp-10-7829-2010).
- Schulz, M, C Textor, S Kinne, Y Balkanski, S Bauer, T Berntsen, T Berglen, O Boucher, F Dentener, S Guibert, ISA Isaksen, T Iversen, D Koch, A Kirkevåg, X Liu, V Montanaro, G Myhre, J Penner, G Pitari, S Reddy, Ø Seland, P Stier, and T Takemura. 2006. “Radiative forcing by aerosols as derived from the AeroCom present-day and pre-industrial simulations.” *Atmospheric Chemistry and Physics* 6: 5225-5246, [doi:10.5194/acp-6-5225-2006](https://doi.org/10.5194/acp-6-5225-2006).
- Seidel, FC and C Popp. 2012. “Critical surface albedo and its implications to aerosol remote sensing.” *Atmospheric Measurement Techniques* 5: 1653-1665, [doi:10.5194/amt-5-1653-2012](https://doi.org/10.5194/amt-5-1653-2012).
- Skamarock, WC, JB Klemp, J Dudhia, DO Gill, DM Barker, MG Duda, X-Y Huang, W Wang, and JG Powers. 2008. *A description of the Advanced Research WRF, Version 3*. NCAR Technical Note NCAR/TN-475+STR, National Center for Atmospheric Research, Boulder, Colorado.
- Soden, BJ and GA Vecchi. 2011. “The vertical distribution of cloud feedback in coupled ocean-atmosphere models.” *Geophysical Research Letters* 38: L12704, [doi:10.1029/2011GL047632](https://doi.org/10.1029/2011GL047632).
- Sorooshian, A, G Feingold, MD Lebsock, H Jiang, and GL Stephens. 2009. “On the precipitation susceptibility of clouds to aerosol perturbations.” *Geophysical Research Letters* 36: L13803, [doi:10.1029/2009GL038993](https://doi.org/10.1029/2009GL038993).
- Sorooshian, A, G Feingold, MD Lebsock, H Jiang, and GL Stephens. 2010. “Deconstructing the precipitation susceptibility construct: improving methodology for aerosol-cloud-precipitation studies.” *Journal of Geophysical Research* 115: D17201, [doi:10.1029/2009JD013426](https://doi.org/10.1029/2009JD013426).
- Stevens, B, C-H Moeng, AS Ackerman, CS Bretherton, A Chlond, S de Roode, J Edwards, J-C Golaz, H Jiang, M Khairoutdinov, MP Kirkpatrick, DC Lewellen, A Lock, F Müller, DE Stevens, E Whelan, and P Zhu. 2005. “Evaluation of large-eddy simulations via observations of nocturnal marine stratocumulus.” *Monthly Weather Review* 133: 1443-1462, [doi:10.1175/MWR2930.1](https://doi.org/10.1175/MWR2930.1).
- Stier, P, NAI Schutgens, N Bellouin, H Bian, O Boucher, M Chin, S Ghan, N Huneeus, S Kinne, G Lin, X Ma, G Myhre, JE Penner, CA Randles, B Samset, M Schulz, T Takemura, F Yu, H Yu, and C Zhou. 2013. “Host model uncertainties in aerosol radiative forcing estimates: results from the AeroCom

prescribed intercomparison study.” *Atmospheric Chemistry and Physics* 13: 3245-3270, [doi:10.5194/acp-13-3245-2013](https://doi.org/10.5194/acp-13-3245-2013).

Swap, RJ, HJ Annegarn, JT Suttles, MD King, S Platnick, JL Privette, and RJ Scholes. 2003. “Africa burning: a thematic analysis of the Southern African Regional Science Initiative (SAFARI 2000).” *Journal of Geophysical Research* 108(D13), [doi:10.1029/2003JD003747](https://doi.org/10.1029/2003JD003747).

Terai, CR, R Wood, DC Leon, and P Zuidema. 2012. “Does precipitation susceptibility vary with increasing cloud thickness in marine stratocumulus?” *Atmospheric Chemistry and Physics* 12 :4567-4583, [doi:10.5194/acp-12-4567-2012](https://doi.org/10.5194/acp-12-4567-2012).

Tridon, F, A Battaglia, P Kollias, E Luke, CR Williams. 2013. “Signal postprocessing and reflectivity calibration of the Atmospheric Radiation Measurement Program 915-MHz wind profilers.” *Journal of Atmospheric and Oceanic Technology* 30: 1038-1054, [doi:10.1175/JTECH-D-12-0066146.1](https://doi.org/10.1175/JTECH-D-12-0066146.1).

Turner, DD and U Loehnert. 2014. “Information content and uncertainties in thermodynamic profiles and liquid cloud properties retrieved from the ground-based Atmospheric Emitted Radiance Interferometer (AERI).” *Journal of Applied Meteorology and Climatology* 53: 752-771, [doi:10.1175/JAMC-D-13-0126.1](https://doi.org/10.1175/JAMC-D-13-0126.1).

Twomey, S. 1977. “The influence of pollution on the shortwave albedo of clouds.” *Journal of Atmospheric Sciences* 34: 1149-1152, [doi:10.1175/1520-0469\(1977\)034<1149:TIOPOT>2.0.CO;2](https://doi.org/10.1175/1520-0469(1977)034<1149:TIOPOT>2.0.CO;2).

Vakkari, V, V-M Kerminen, JP Beukes, P Tiitta, PG van Zyl, M Josipovic, AD Venter, K Jaars, DR Worsnop, M Kulmala, and L Laakso. 2014. “Rapid changes in biomass burning aerosols by atmospheric oxidation.” *Geophysical Research Letters* 41: 2644-2651, [doi:10.1002/2014GL059396](https://doi.org/10.1002/2014GL059396).

van der Werf, GR, JT Randerson, L Giglio, GJ Collatz, PS Kasibhatla, and AF Arellano Jr. 2006. “Interannual variability in global biomass burning emissions from 1997 to 2004.” *Atmospheric Chemistry and Physics* 6: 3423-3441, [doi:10.5194/acp-6-3423-2006](https://doi.org/10.5194/acp-6-3423-2006).

van der Werf, GR, JT Randerson, L Giglio, GJ Collatz, M Mu, PS Kasibhatla, DC Morton, RS DeFries, Y Jin, and TT van Leeuwen. 2010. “Global fire emissions and the contribution of deforestation, savanna, forest, agricultural, and peat fires (1997-2009).” *Atmospheric Chemistry and Physics* 10: 11707-11735, [doi:10.5194/acp-10-11707-2010](https://doi.org/10.5194/acp-10-11707-2010).

Voigt, BS, S Bony, and O Boucher. 2013. “Easy aerosol: a modeling framework to study robustness and sources of uncertainties in aerosol-induced changes of the large-scale atmospheric circulation.” Available through wcrp-climate.org/index.php/gc-clouds-circulation-activities/gc4-clouds-initiatives/368-gc-clouds-initiative3-easy-aerosol.

Wang, H and G Feingold. 2009a. “Modeling mesoscale cellular structures and drizzle in marine stratocumulus. Part I: impact of drizzle on the formation and evolution of open cells.” *Journal of Atmospheric Sciences* 66: 3237-3256, [doi:10.1175/2009JAS3022.1](https://doi.org/10.1175/2009JAS3022.1).

Wang, H and G Feingold. 2009b. “Modeling mesoscale cellular structures and drizzle in marine stratocumulus. Part II: the microphysics and dynamics of the boundary region between open and closed cells.” *Journal of Atmospheric Sciences* 66: 3257-3275, [doi:10.1175/2009JAS3120.1](https://doi.org/10.1175/2009JAS3120.1).

- Wang, H, WC Skamarock, and G Feingold. 2009. "Evaluation of scalar advection schemes in the Advanced Research WRF Model using large-eddy simulations of aerosol-cloud interactions." *Monthly Weather Review* 137: 2547-2558, [doi:10.1175/2009MWR2820.1](https://doi.org/10.1175/2009MWR2820.1).
- Wang H, G Feingold, R Wood, and J Kazil. 2010. "Modeling microphysical and meteorological controls on precipitation and cloud cellular structures in Southeast Pacific stratocumulus." *Atmospheric Chemistry and Physics* 10(13): 6347-6362, [doi:10.5194/acp-10-6347-2010](https://doi.org/10.5194/acp-10-6347-2010).
- Wang, H, RC Easter, PJ Rasch, M Wang, X Liu, SJ Ghan, Y Qian, J-H Yoon, P-L Ma, and V Vinoj. 2013. "Sensitivity of remote aerosol distributions to representation of cloud-aerosol interactions in a global climate model." *Geoscientific Model Development* 6: 765-782, [doi:10.5194/gmd-6-765-2013](https://doi.org/10.5194/gmd-6-765-2013).
- Wang, H, PJ Rasch, RC Easter, B Singh, R Zhang, P-L Ma, Y Qian, SJ Ghan, and N Beagley. 2014. "Using an explicit emission tagging method in global modeling of source-receptor relationships for black carbon in the Arctic: variations, sources, and transport pathways." *Journal of Geophysical Research: Atmospheres* 119: 12888-12909, [doi:10.1002/2014JD022297](https://doi.org/10.1002/2014JD022297).
- Wang, M, S Ghan, X Liu, TS L'Ecuyer, K Zhang, H Morrison, M Ovchinnikov, R Easter, R Marchand, D Chand, Y Qian, and JE Penner. 2012. "Constraining cloud lifetime effects of aerosols using A-Train satellite observations." *Geophysical Research Letters* 39: L15709, [doi:10.1029/2012GL052204](https://doi.org/10.1029/2012GL052204).
- Waquet, F, F Peers, F Ducos, P Goloub, S Platnick, J Riedi, D Tanre, and F Thieuleux. 2013. "Global analysis of aerosol properties above clouds." *Geophysical Research Letters* 40: 5809-5814, [doi:10.1002/2013GL057482](https://doi.org/10.1002/2013GL057482).
- Welton, EJ, JR Campbell, JD Spinhirne, and VS Scott. 2001. "Global monitoring of clouds and aerosols using a network of micropulse lidar systems", in "Lidar Remote Sensing for Industry and Environmental Monitoring." UN Singh, T Itabe, and N Sugimoto (eds.), *Proceedings of SPIE*, 4153: 151-158, [doi:10.1117/12.417040](https://doi.org/10.1117/12.417040).
- Wen, G, A Marshak, RF Cahalan, LA Remer, and RG Kleidman. 2007. "3-D aerosol-cloud radiative interaction observed in collocated MODIS and ASTER images of cumulus cloud fields." *Journal of Geophysical Research* 112: D13204, [doi:10.1029/2006JD008267](https://doi.org/10.1029/2006JD008267).
- Wilcox, EM. 2010. "Stratocumulus cloud thickening beneath layers of absorbing smoke aerosol." *Atmospheric Chemistry and Physics* 10: 11769-11777, [doi:10.5194/acp-10-11769-2010](https://doi.org/10.5194/acp-10-11769-2010).
- Wilcox, EM. 2012. "Direct and semi-direct radiative forcing of smoke aerosols over clouds." *Atmospheric Chemistry and Physics* 12: 139-149, [doi:10.5194/acp-12-139-2012](https://doi.org/10.5194/acp-12-139-2012).
- Wood, R. 2007. "Cancellation of aerosol indirect effects in marine stratocumulus through cloud thinning." *Journal of Atmospheric Sciences* 64: 2657-2669, [doi:10.1175/JAS3942.1](https://doi.org/10.1175/JAS3942.1).
- Wood, R, M Wyant, CS Bretherton, J Rémillard, P Kollias, J Fletcher, J Stemmler, S deSzoeko, S Yuter, M Miller, D Mechem, G Tselioudis, JC Chiu, JAL Mann, EJ O'Connor, RJ Hogan, X Dong, M Miller, V Ghate, A Jefferson, Q Min, P Minnis, R Palinkonda, B Albrecht, E Luke, C Hannay, and Y Lin. 2015. "Clouds, aerosols, and precipitation in the marine boundary layer: an ARM Mobile Facility deployment." *Bulletin of the American Meteorological Society* 96: 419-440, [doi:10.1175/BAMS-D-13-00180.1](https://doi.org/10.1175/BAMS-D-13-00180.1).

- Wyant, MC, CS Bretherton, A Chlond, BM Griffin, H Kitagawa, C-L Lappen, VE Larson, A Lock, S Park, SR de Roode, J Uchida, M Zhao, and AS Ackerman. 2007. "A single-column model intercomparison of a heavily drizzling stratocumulus-topped boundary layer." *Journal of Geophysical Research* 112: D24204, [doi:10.1029/2007JD008536](https://doi.org/10.1029/2007JD008536).
- Yang, Q, WI Gustafson Jr., JD Fast, H Wang, RC Easter, H Morrison, Y-N Lee, EG Chapman, SN Spak, and MA Mena-Carrasco. 2011. "Assessing regional scale predictions of aerosols, marine stratocumulus, and their interactions during VOCALS-REx using WRF-Chem." *Atmospheric Chemistry and Physics* 11: 11951-11975, [doi:10.5194/acp-11-11951-2011](https://doi.org/10.5194/acp-11-11951-2011).
- Yang, Q, WI Gustafson Jr., JD Fast, H Wang, RC Easter, M Wang, SJ Ghan, LK Berg, LR Leung, and H Morrison. 2012. "Impact of natural and anthropogenic aerosols on stratocumulus and precipitation in the Southeast Pacific: A regional modeling study using WRF-Chem." *Atmospheric Chemistry and Physics* 12: 8777-8796, [doi:10.5194/acp-12-8777-2012](https://doi.org/10.5194/acp-12-8777-2012).
- Zhang, J and JS Reid. 2010. "A decadal regional and global trend analysis of the aerosol optical depth using data-assimilation grade over-water MODIS and Level 2 MISR aerosol products." *Atmospheric Chemistry and Physics* 10: 10949-10963, [doi:10.5194/acp-10-10949-2010](https://doi.org/10.5194/acp-10-10949-2010).
- Zhang, MH and JL Lin. 1997. "Constrained variational analysis of sounding data bases on column-integrated budgets of mass, heat, moisture, and momentum: approach and application to ARM measurements." *Journal of Atmospheric Sciences* 54: 1503-1524, [doi:10.1175/1520-0469\(1997\)054<1503:CVAOSD>2.0.CO;2](https://doi.org/10.1175/1520-0469(1997)054<1503:CVAOSD>2.0.CO;2).
- Zhang, MH, JL Lin, RT Cederwall, JJ Yio, and SC Xie. 2001. "Objective analysis of ARM IOP data: method and sensitivity." *Monthly Weather Review* 129(2): 295-311, [doi:10.1175/1520-0493\(2001\)129<0295:OAOAID>2.0.CO;2](https://doi.org/10.1175/1520-0493(2001)129<0295:OAOAID>2.0.CO;2).
- Zhu, P, CS Bretherton, M Koehler, A Cheng, A Chlond, Q Geng, P Austin, J-C Golaz, G Lenderink, A Lock, and B Stevens. 2005. "Intercomparison and interpretation of single-column model simulations of a nocturnal stratocumulus-topped marine boundary layer." *Monthly Weather Review* 133: 2741-2758, [doi:10.1175/MWR2997.1](https://doi.org/10.1175/MWR2997.1).
- Zuidema, P, H Xue, and G Feingold. 2008. "Shortwave radiative impacts from aerosol effects on marine shallow cumuli." *Journal of Atmospheric Sciences* 65: 1979-1990, [doi:10.1175/2007JAS2447.1](https://doi.org/10.1175/2007JAS2447.1).
- Zuidema, P, Z Li, RJ Hill, L Bariteau, B Rilling, C Fairall, WA Brewer, B Albrecht, and J Hare. 2012. "On trade-wind cumulus cold pools." *Journal of Atmospheric Sciences* 69: 258-280, [doi:10.1175/JAS-D-11-0143.1](https://doi.org/10.1175/JAS-D-11-0143.1).



U.S. DEPARTMENT OF
ENERGY

Office of Science